EXPERIMENTAL EVOLUTION OF ONCOLYTIC VESICULAR STOMATITIS VIRUSES IN CANCER CELLS

by

Sara Louise Nickel Seegers

A thesis submitted to the faculty of
The University of North Carolina at Charlotte
in partial fulfillment of the requirements
for the degree of Master of Science in
Biological Sciences

Charlotte

2019

Approved by:

_____
Dr. Valery Grdzelishvili

_____
Dr. Didier Dréau

_____
Dr. Andrew Truman

ABSTRACT

SARA LOUISE NICKEL SEEGERS. Experimental of oncolytic vesicular stomatitis viruses in cancer cells. (Under the direction of DR. VALERY GRDZELISHVILI)

Vesicular stomatitis virus (VSV) based oncolytic viruses are promising agents against various cancers. We have shown that pancreatic ductal adenocarcinoma (PDAC) cell lines exhibit great diversity in susceptibility and permissibility to VSV. Here, we analyzed if PDAC resistance to VSV could be decreased by directed viral evolution using our two previously described oncolytic VSV recombinants, VSV-p53wt and VSV-p53-CC. Each virus encodes VSV matrix protein with ΔM51 mutation (M-ΔM51) and one of two versions of a functional human tumor suppressor p53 fused to a fluorescent reporter protein eqFP650. Each virus was serially passaged 32 times (accounts for more than 60 viral replication cycles) on either SUIT-2 (moderately resistant to VSV) or MIA PaCa-2 (highly permissive to VSV) human PDAC cell lines. While no phenotypic changes were observed for MIA PaCa-2-passaged viruses, both SUIT-2-passaged VSV-p53wt and VSV-p53-CC showed improved replication in SUIT-2 and another PDAC cell line AsPC-1 (moderately resistant to VSV), while remaining highly attenuated in non-malignant cell lines. Surprisingly, two identical VSV glycoprotein (G) mutations, E238K and K174E were identified in both SUIT-2-passaged viruses. Additional experiments indicated that the acquired G mutations improved VSV replication at least in part due to improved virus attachment to SUIT-2 cells. Importantly, no mutations were found in the M-ΔM51 protein and no deletions or mutations were found in the p53 or eqFP650 portions of virus-encoded transgenes in any of the passaged viruses. These findings demonstrate long-term genomic

stability of complex VSV recombinants encoding large transgenes, and support further clinical development of oncolytic VSV recombinants as safe cancer therapeutics.

DEDICATION

To my parents, Lisa and Patrick Seegers

and

my grandparents, Edward and Sylvia Nickel.

ACKNOWLEDGMENTS

This work was made possible by the mentorship of Dr. Valery Grdzelishvili, thank you for your guidance and the opportunity to work in your lab. I would like to thank my committee members, Dr. Didier Dréau, and Dr. Andrew Truman for their important feedback and guidance. Thank you to members of the Grdzelishvili lab, Dr. Sebastien Felt, Dr. Christian Bressy, Gaith Droby, Dakota Goad, Bryant Maldonado, Sarah Greene, Connor Frasier, Christopher Castagno, Ben Hall, and Mohamad Hajjar for your technical assistance, moral support, and friendship throughout my graduate career. Thank you to Dr. Irina Nesmelova for providing expertise in protein modeling and to the following laboratories for kindly providing reagents for this project: Jack Rose (Yale University) for VSV-ΔM51; Michael Hollingsworth (University of Nebraska Medical Center) for SUIT-2 cells; Pinku Mukherjee (University of North Carolina at Charlotte) for MIA PaCa-2.

I would like to thank Max Rogers, Laura Knighton, Amanda Luzadre, and Leah Painter for their support during my time in graduate school which has been truly invaluable.

I would like to thank the UNCC Center for Biomedical Engineering and Science (CBES) for summer and conference travel support. This research was supported by V.Z.G's grants. 1R15CA195463-01A1 and 1R15CA238864-01 from the National Cancer Institute, National Institutes of Health (Bethesda, Maryland, USA).

TABLE OF CONTENTS

LIST OF TABLES x

LIST OF FIGURES xi

LIST OF ABBREVIATIONS xii

CHAPTER 1: INTRODUCTION 1

1.1 Background 1

1.1.1 Vesicular Stomatitis Virus 2

1.1.2 Oncolytic Virotherapy Overview 5

1.1.3 VSV as an OV 6

1.1.4 Transgenic Oncolytic Virotherapy 7

1.1.5 Directed Evolution Approach 9

1.1.6 Pancreatic Ductal Adenocarcinoma 10

1.2 Rationale 11

CHAPTER 2: HYPOTHESES AND SPECIFIC AIMS 13

2.1 Hypotheses 13

2.2 Research Focus 13

2.3 Specific Aims 13

CHAPTER 3: DIRECTED EXPERIMENTAL EVOLUTION OF VSV AND THE CHARACTERIZATION OF NOVEL VSV MUTANTS 14

3.1 Materials and Methods 14

3.1.1 Viruses and cell lines 14

3.1.2 Viral Passaging 15

3.1.3 RNA isolation, cDNA generation, PCR amplification, and DNA sequence analysis 16

3.1.4 Viral replication kinetics assay and crystal violet cytotoxicity assay 17

3.1.5 Western blot analysis 17

3.1.6 Virion attachment assay 18

3.1.7 Virus Purification 19

3.1.8 Inhibition of VSV infection with soluble LDLR 20

3.1.9 Effects of DEAE-Dextran on VSV p53wt (Founder) and VSV-p53wt (SUIT-2) infectivity and replication 20

3.2 Results 21

3.2.1 Experimental evolution of two oncolytic VSV variants in two human PDAC cell lines 21

3.2.2 Viral genome sequence analysis of passaged viruses 21

3.2.3 Stability of transgenes over extensive viral passaging 22

3.2.4 Identification of 2 identical mutations in suit-2 passaged viruses 23

3.2.5 Identification of a third mutation in VSV-P53-CC (SUIT-2) 24

3.2.6 SUIT-2 passaged viruses show an improved replication in PDAC cells, while retaining their oncoselectivity 24

3.2.7 K174E is required for an improved replication of VSV experimentally evolved in SUIT-2 cells 25

3.2.8 Acquired G mutations do not inhibit antiviral signaling and retain oncoselectivity 26

3.2.9 Acquired G mutations improve attachment to SUIT-2 cells 28

3.2.10 SUIT-2 adapted viruses are still able to interact with LDLR 29

3.2.11 Treatment with DEAE-dextran does not improve SUIT-2 adapted viruses replication in SUIT-2 cells 30

3.2.12 E238K and K174E location analysis in pre and post-fusion 31

3.3 Figures and Tables 33

3.4 Discussion 53

CHAPTER 4: CONCLUSION 64

REFERENCES 67

LIST OF TABLES

TABLE 1: Primers used for VSV PCR amplification and sequencing 34

LIST OF FIGURES

FIGURE 1: Structure and genome of wild type VSV. 5

FIGURE 2: Scheme of viral passaging. 33

FIGURE 3: Examination of transgene stability and sequencing of viral genomes. 35

FIGURE 4: The chronological order of the appearance of VSV-G mutations E238K and K174E during passaging of viruses on SUIT-2 cells. 37

FIGURE 5: Chronological appearance of M184I mutation in VSV-p53-CC (SUIT-2). 38

FIGURE 6: Viral replication kinetics of the founder and Passage 33 viruses. 39

FIGURE 7: Crystal violet cytotoxicity assay. 40

FIGURE 8: Generation and replication of single and double mutant plaque isolated viruses. 41

FIGURE 9: Replication of the founder and passage 33 viruses in different cell lines. 43

FIGURE 10: Replication of single and double mutant plaque isolated viruses in different cell lines to examine oncoselectivity. 44

FIGURE 11: Comparing VSV attachment and replication in BHK-21 and SUIT-2 cells. 46

FIGURE 12: Effect of sLDLR on infectivity of VSV-p53wt viruses with WT G, Single Mutant (E238K) G and Double Mutant (K174E/E238K) G. 48

FIGURE 13: Effect of polycation DEAE-dextran on VSV infection in different cell lines. 50

FIGURE 14: Sequence comparison of WT VSV-G and mutant VSV-G. 51

FIGURE 15: Location of VSV-G E238K and K174E mutations on crystallographic structures of pre-fusion and post-fusion states of the glycoprotein G. 52

LIST OF ABBREVIATIONS

CC- coiled-coil

CNS- central nervous system

ds- double stranded

G- glycoprotein

h- hours

RFP- red fluorescent protein

IFN- interferon

L- large polymerase protein

LDLR- low-density lipoprotein receptor

M- matrix protein

M51- deletion of the methionine at position 51

MOI- multiplicity of infection

N- nucleocapsid protein

NNS- nonsegmented negative-strand

Nt- nucleotide

OV- oncolytic virus

PDAC- pancreatic ductal adenocarcinoma

p.i.- post infection

PS- phosphatidylserine

RdRp- RNA dependent RNA polymerase

ss- single stranded

STAT- signal transducer and activator of transcription

VSV- vesicular stomatitis virus

WT- wild type

CHAPTER 1: INTRODUCTION

1.1 Background

Viruses, the most abundant biological entities on earth, are submicroscopic, obligate intracellular parasites comprised of nucleic acid wrapped in a protein coat in their most basic form (Koonin, 2010; Perlmutter and Hagan, 2015). The protein coat that packages a viral genome is called a capsid. Some viruses contain another outer layer called an envelope which is a lipid bilayer that is derived from the host cells own membrane. The capsid or virus envelope play important roles in viral interactions with host cells as this is the surface that will be in direct contact with the cell membrane. These layers also provide protection from the external environment that could damage the viral genome. The Baltimore classification of viruses established by David Baltimore classifies viruses into 7 different families based on their type of genome and how they replicate their genome. These groups are: I (double stranded (ds) DNA genome), II (single stranded (ss) DNA genome), III (dsRNA genome), IV (ssRNA positive strand genome), V (ssRNA negative-strand genome), VI (ssRNA positive-strand genome, reverse transcriptase), VII (dsRNA, reverse transcriptase) (Baltimore, 1971). While viruses can cause harm to the organisms they infect, they are also beneficial as they have led to many discoveries in biological research and are even used as therapeutical agents in the form of vaccine development, gene therapy, bacteriophage therapy, and cancer therapy (Draper and Heeney, 2010; Felt and Grdzelishvili, 2017; Thomas et al., 2003) (Lin et al., 2017; Russell et al., 2012) (Verma and Weitzman, 2005).

Oncolytic virus (OV) therapy is an emerging approach utilizing viruses that preferentially infect and kill cancer cells. While OV therapy has had pre-clinical and

clinical success, there are limitations such as cancers being resistant to OV therapy. Our lab focuses on vesicular stomatitis virus (VSV) as on OV for pancreatic ductal adenocarcinoma (PDAC) and this work focuses specifically on improving VSV as an OV through a directed experimental approach while simultaneously investigating the stability of transgenes within VSVs genome over the course of extensive viral passaging.

1.1.1 Vesicular Stomatitis Virus

VSV is a prototypic nonsegmented negative-strand (NNS), RNA virus (order *Mononegavirales*, family *Rhabdoviridae*, genus *Vesiculovirus*). Multiple strains of VSV exist however the 2 most common are VSV New Jersey and VSV Indiana (Martinez and Wertz, 2005). VSV most commonly infects mammals such as cattle and rodents resulting in sores on the mouth and feet of infected individuals throughout regions of North, Central, and South America. VSV can also infect human hosts however the symptoms are usually much less severe (Tesh et al., 1969). VSV has neurotropic tendencies as the central nervous system (CNS) lacks a robust immune response and CNS neurons do not replicate (Paul et al., 2007). VSVs neurotropism has been documented in both murine and non-human primate models through intranasal or intracranial infection (Johnson JE et al., 2007) (van den Pol et al., 2002). The neurotoxicity associated with VSV infection administered intranasally has been well studied and results in VSV replication in the nasal epithelium which moves to the olfactory neurons and finally retrograde axonally to replicate in the brain which results in encephalitis (Bi et al., 1995) (Reiss et al., 1998) (van den Pol et al., 2002).

VSV is able to infect a wide range of hosts and replicate in a wide range of cell types (Hastie et al., 2013) due to ubiquitously expressed cell-surface receptors that can be

used by the virus. The low-density lipoprotein receptor (LDLR) and other members of the LDLR family have been shown to serve as VSV receptors (Amirache et al., 2014; Ammayappan et al., 2013; Finkelshtein et al., 2013; Nikolic et al., 2018), and additional studies showed that other cell surface molecules, such as phosphatidylserine (Carneiro et al., 2006; Coil and Miller, 2004; Schlegel et al., 1983), sialoglycolipids (Schloemer and Wagner, 1975), and heparan sulfate (Guibinga et al., 2002) could also play a role in VSV attachment to host cells. VSV-G is the viral protein responsible for attachment and entry into host cells through the interaction with the previously mentioned known receptors on the host cells surface. VSV-G contains 2 sites that are post translationally glycosylated which have been shown to play a role in cell infection depending on the cell line being infected however other non-specific interactions between the virus and host cell that alter the efficacy of VSV attachment to host cells (Bailey et al., 1989; Hastie et al., 2013; Machamer et al., 1985; Robertson et al., 1976). Treatment with polycations has been shown to improve VSV attachment to host cells most likely by decreasing electrostatic repulsion between the negatively charged viral envelope and the negatively charged cell membrane (Bailey et al., 1984; Conti et al., 1991). After VSV attaches to a host cell via specific and non-specific interactions, VSV is endocytosed into the host cell. Fusion of the viral envelope with the endosomal membrane occurs when pH decreases in the endosomal vesicle resulting in a conformational shift in VSV-G that is responsible for the fusion of membranes. which in turn releases the viral nucleocapsid into cells cytoplasm. Since VSV has a negative sense RNA genome, its genome must first be transcribed to mRNA from which viral proteins can be synthesized and assembled with the replicated negative sense RNA viral genome. Once new progeny virions are assembled, they bud

from the host cells plasma membrane which VSV-G has been incorporated into, which is where the new VSV virions gain their envelope. Host cell must be permissive and able to support each step of the virus replication cycle to result in infectious viral progeny and different cell lines result in differing amounts of virion production depending on their permissiveness to the viral infection.

VSV is a well characterized virus widely used in studies involving gene therapy, vaccine development, and oncolytic virotherapy (Bukreyev et al., 2006; Finke and Conzelmann, 2005; Ke et al., 2019; von Messling V and Cattaneo, 2004). VSV is an enveloped, bullet shaped virus consisting of an 11-kb genome that encodes five proteins: nucleocapsid protein (N), phosphoprotein (P), matrix protein (M), glycoprotein (G), and large polymerase (L) (Lyles DS, 2007). The VSV-N protein encapsidates the VSV genome which forms a nuclease resistant N-RNA complex. This complex associates with the VSV-L and VSV-P proteins which form viral RNA-dependent RNA polymerase (RdRp) which is responsible for transcribing the viral genome. The N-RNA complex associated with the RdRp complex is called the viral ribonucleoprotein complex (RNP) and the RNP is surrounded by VSV-M. VSV-M plays an important role in the inhibition of the innate immune response to prevent clearance of the virus from the host cell (Ahmed et al., 2003). This VSV-M covered RNP is encapsulated by the viral envelope which VSV-G is embedded in with VSV-G being the viral protein responsible for attachment and entry into host cells (Fig.1) (Lyles DS, 2007).

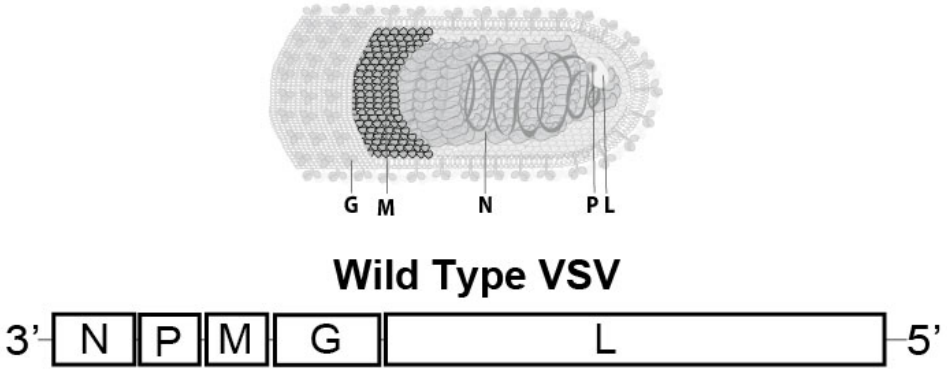

Figure 1: Wild type VSV virion structure and genome. VSV has a non-segmented negative sense RNA genome that encodes 5 genes: N, P, M, G, L that assemble as an enveloped, bullet-shaped virion. Adapted from Hastie et.al.

1.1.2 Oncolytic Virotherapy Overview

Many viruses inherently preferentially infect, replicate in and kill cancer cells. Naturally occurring or engineered viruses that preferentially kill cancer cells have been termed oncolytic viruses (OVs). The oncoselectivity of most OVs, including VSV, is based mainly on defective or reduced type I IFN responses in cancer cells (Balachandran and Barber, 2004; Barber, 2004; Lichty BD et al., 2004; Marozin et al., 2008; Marozin et al., 2010; Moussavi et al., 2010; Stojdl DF et al., 2003; Stojdl et al., 2000; Zhang et al., 2010), compared to non-malignant ("normal") cells. These responses are generally unfavorable for tumor development as they are anti-proliferative, anti-angiogenic, and pro-apoptotic (Wang et al., 2011a). Oncolytic viruses have been of interest since the 19th century when researchers first observed naturally acquired viruses ability to regress tumor development in patients, however, there was limited success with viruses as a treatment for cancer as the oncoselectivity, or specificity for only malignant cells, of the viruses was lacking and in immunocompetent patients the OV would be cleared by the immune system before the virus was able decrease tumor growth (Kelly and Russell,

2007). Through modern biotechnology, viruses have been engineered to improve oncolytic virotherapy. One such way OVs oncoselectivity has been refined is by exploiting viruses susceptibility to innate immune responses elicited by non-malignant cells (Ayala-Breton et al., 2013). Viruses can also be engineered to target biomarkers of malignant cells more specifically to improve oncoselectivity (Freedman et al., 2018). Engineered OVs have had pre-clinical and clinical success with three OVs currently approved to be used in clinical settings for melanoma treatment: 1. enteric cytopathic human orphan virus 7 based RIGVIR was approved for clinical treatment use in Georgia, Armenia, and Latvia in 2015, 2. herpes simplex virus 1 based OV and 3.T-VEC, which was approved in the USA and European Union in 2016. For the treatment of head and neck squamous cell carcinoma, adenovirus type 5 based Gendicine and Oncorine was approved in China in 2006.

1.1.3 VSV as an OV

VSV specifically is a promising oncolytic virus (OV) due to its inherent ability to preferentially replicate in cancer cells and because of a lack of preexisting immunity against VSV in the human population (Felt and Grdzelishvili, 2017; Hastie and Grdzelishvili, 2012; Simovic et al., 2015). Although wild-type (WT) VSV is sensitive to type I IFN mediated antiviral responses in most normal tissues, WT VSV-M sufficiently inhibits type I IFN responses to allow viral replication in the central nervous system (CNS) (Clarke DK, 2007; Johnson JE et al., 2007). However, due to a well-established reverse-genetics system available for VSV, a large number of safe oncoselective VSV-based oncolytic viruses have been generated and tested in numerous studies (Felt and Grdzelishvili, 2017; Hastie and Grdzelishvili, 2012). Some of the most widely used

oncolytic VSVs are recombinants carrying a deletion (M-ΔM51) or substitution (M51R) of methionine at amino acid (aa) residue 51 in VSV-M. These mutations attenuate VSV replication in normal cells by preventing WT VSV-M protein from inhibition the nuclear exit of host mRNAs, including transcripts for virus-induced antiviral genes (Black and Lyles, 1992; Black et al., 1993; Coulon et al., 1990). As a result, unlike WT VSV, VSV M51 mutants have dramatically attenuated neurotoxicity but retain robust oncolytic abilities (Ahmed et al., 2003; Brown et al., 2009; Ebert O et al., 2005; Stojdl DF et al., 2003; Trottier et al., 2007; von Kobbe et al., 2000; Wollmann G et al., 2010).

1.1.4 Transgenic Oncolytic Virotherapy

A common approach to generate safe oncolytic VSV is to introduce a transgene improving oncoselectivity or/and induction of adaptive anti-tumor immune responses (Felt and Grdzelishvili, 2017; Hastie and Grdzelishvili, 2012; Simovic et al., 2015). For example, previous studies showed that functional human tumor suppressor p53 variants can be successfully integrated into VSV genome (Hastie et al., 2015; Heiber and Barber, 2011). Our laboratory generated two recombinants, VSV-p53wt and VSV-p53-CC, each expressing M-ΔM51 and a different version of a functional tumor suppressor p53 fused to a near-infrared fluorescent protein eqFP650 (hereinafter referred to as RFP) (Hastie et al., 2015). While WT p53 is a powerful tumor suppressor, it can become a devastating oncogene once mutated, mostly via missense mutations, which should be considered when incorporated into anti-cancer therapies (Kandoth et al., 2013). VSV-p53wt encodes a human WT p53, while VSV-p53-CC encodes a human p53 with its tetramerization domain substituted with the coiled-coil (CC) domain of breakpoint cluster region (Bcr) protein (Okal et al., 2013). The resulting p53-CC protein evades the dominant-negative activities

of endogenously expressed mutant p53 (Okal et al., 2013). Our previous study showed that these VSV-encoded p53 transgenes not only enhanced VSV anti-cancer abilities through the introduction of functional p53 into cancer cells with defective tumor suppression activity, but also through the downregulation of antiviral signaling in cancer cells, while stimulating it in normal cells (Hastie et al., 2015).

As a result of the numerous preclinical studies demonstrating the effectiveness of different VSV recombinants as OVs (Felt and Grdzelishvili, 2017; Hastie and Grdzelishvili, 2012; Russell et al., 2012), VSV-hIFNbeta-NIS, encoding the human cytokine interferon beta (hIFNbeta) and the human thyroidal sodium-iodine symporter (NIS), is currently being tested in the United States in several phase I clinical trials against various malignancies (see details for trials NCT02923466, NCT03120624, and NCT03017820).

Despite these advances, many challenges exist regarding the use of VSV as an oncolytic virus in clinic. For example, not all tumors are susceptible and/or permissive to VSV (Felt and Grdzelishvili, 2017; Hastie and Grdzelishvili, 2012). Our previous studies showed that pancreatic ductal adenocarcinoma (PDAC) cell lines show great diversity in susceptibility and permissibility to VSV based OVs, such as VSV-ΔM51. We previously identified several mechanisms behind resistance of PDACs to VSV-based therapy, such as abnormal or residual type I IFN antiviral activities (Cataldi et al., 2015; Hastie et al., 2016; Moerdyk-Schauwecker et al., 2013; Murphy et al., 2012), inefficient attachment of VSV to some PDACs (Felt et al., 2017), and resistance of VSV-infected PDAC cells to virus-mediated apoptosis (Felt et al., 2015).

Another potential problem is that VSV, as any other RNA virus, can mutate rapidly due to the lack of proofreading activities in virus-encoded RNA-dependent RNA polymerase (RdRp) (Steinhauer et al., 1992). Such spontaneous mutations could revert attenuated VSV back to a WT phenotype. For example, in the case of VSV-ΔM51 recombinants, secondary mutations in VSV-M could hypothetically restore WT M functions and reduce VSV-ΔM51 oncoselectivity. Also, VSV has a small RNA genome, and the addition of any transgenes typically attenuates viral replication as the added genetic information hinders speed of viral genome replication and attenuates transcription of downstream viral genes (Wertz et al., 2002). A spontaneous loss of a transgene, particularly if the transgene is the attenuating factor, is an undesirable possibility. Another hypothetical complication is single site mutations in the beneficial transgene, which could completely negate or change its function resulting in an ineffective or potentially pathogenic function. Despite VSV being an RNA virus that can mutate rapidly, there is evidence that VSVs genome remains relatively stable in endemic regions (Letchworth et al., 1999).

1.1.5 Directed Evolution Approach

One method to improve VSV as an OV against resistant cell lines is a directed viral evolution approach where OVs are serially passaged on a target malignant cell line to allow the virus to acquire mutations that enable it to replicate and kill the target cell line better. Directed evolution and bioselection for more potent oncolytic viruses has been explored in other studies using a variety of oncolytic viruses and cancer types (Bauzon and Hermiston, 2012; Kuhn et al., 2017; Kuhn et al., 2008; Sanjuan and Grdzelishvili, 2015; Svyatchenko et al., 2017; Yan et al., 2003; Zainutdinov et al., 2019). VSV has been

a widely used model to study viral evolution for several decades (Novella, 2003) and has been experimentally evolved for various purposes such as understanding how viruses evade innate immune responses (Hernandez-Alonso et al., 2015), the generation of novel VSV-G protein variants used to pseudotype retroviral and lentiviral vectors for gene delivery (Yu and Schaffer, 2006), and to produce novel variants of foreign genes encoded in VSV genome (Davis and van den Pol, 2010). Moreover, several previous studies have successfully used a directed evolution approach to improve VSVs oncolytic abilities (Gao et al., 2006; Garijo et al., 2014; Janelle et al., 2011; Wollmann G, 2005).

1.1.6 Pancreatic Ductal Adenocarcinoma

Pancreatic ductal adenocarcinoma (PDAC) is a highly aggressive form of pancreatic cancer that comprises 90% of pancreatic cancers and is the 4th leading cause of cancer related deaths worldwide (Adamska et al., 2017). PDAC is usually not diagnosed until already in later stages when surgical resection is not a viable option and currently has a 5-year survival rate of 7% (Stark et al., 2016). Current clinical practice most commonly treats PDAC with chemoradiotherapy and/or the chemotherapeutics gemcitabine and *nab*-paclitaxel however, PDACs are notoriously chemoresistant making them difficult to treat and often result in poor patient prognosis. This makes it necessary to find new and innovative ways to treat this form of cancer (Swayden et al., 2018; Wang et al., 2011b; Wolfgang et al., 2013). PDAC is often associated with mutations in the RAS genes which consist of the HRAS, KRAS, and NRAS genes. Mutations within KRAS in particular are associated with the initiation of pancreatic cancer being found in more than 90% of PDAC cases (Giri et al., 2017). RAS plays important roles in cell proliferation, differentiation and regulation of apoptosis and mutations in KRAS at

codons 12 and 13 most commonly result in KRAS remaining constitutively activated resulting in the progression of PDAC (Sinn et al., 2014). Other mutations associated with the progression of PDAC are tumor suppressor genes CDKN2A, TP53, and SMAD4 (Rice and Del Rio Hernandez, 2019). VSV based oncolytic viruses are promising agents against PDACs (Wennier et al., 2011) however, some PDAC cell lines are resistant to VSV (Hastie et al., 2016). Multiple mechanisms can be used to lessen or break resistance to OV therapy such as the directional experimental evolution method examined in this thesis.

1.2 Rationale

Pancreatic ductal adenocarcinomas are associated with being highly aggressive, invasive and resistant to chemotherapy. PDAC is often not diagnosed until in later stages due to its lack of external symptoms resulting in limited treatment options. Vesicular stomatitis virus (VSV) based oncolytic viruses are promising agents against PDAC however not ubiquitously, some PDAC cell lines are resistant to VSV. This thesis examined how stable transgenes and the ΔM51 attenuation are within oncolytic VSV-p53wt and VSV-p53-CC genomes over extensive passaging on PDAC cell lines of differing resistances to VSV. This thesis also examined if these viruses can be directionally evolved to better replicate in and kill the PDAC cell line they were extensively passaged on. To understand both the stability and flexibility of VSV as on OV for PDAC treatment is critical. The knowledge gained from extensively passaging oncolytic VSV on malignant cell lines will help to elucidate any potential concerns with the use of oncolytic VSV long-term in a clinical setting. The study will also provide useful information about how to improve OV therapy through the method of directed

evolution. While this work is specific to VSV and PDAC, it will likely be relevant to other OVs and cancers.

CHAPTER 2: HYPOTHESES AND SPECIFIC AIMS

2.1 Hypotheses

1. Complex VSV recombinants are able to stably express transgenes over the course of extensive viral passaging.

2. VSV-p53 can be directionally adapted to replicate better in a resistant PDAC cell line and become more cytotoxic to the cell line it is passaged on.

2.2 Research Focus

Understanding and exploiting long-term evolution of transgene expressing oncolytic vesicular stomatitis virus in pancreatic cancer cells.

2.3 Specific Aims

AIM 1: Passage viruses 33 times and complete genomic sequence analysis of founder and passage 33 viruses.

AIM 2: Investigate oncolytic potential of mutant passage 33 viruses compared to founder viruses.

AIM 3: Investigate the effect of the identified mutations on virus replication cycle.

CHAPTER 3: PASSAGING, SEQUENCE ANALYSIS, AND RETENTION OF TRANSGENES OF DIRECTIONALLY EVOLOVED VIRUSES

3.1 Materials and Methods

3.1.1 Viruses and cell lines

The recombinant viruses VSV-p53wt and VSV-p53-CC were previously engineered using the VSV-ΔM51 backbone and were previously described in detail (Hastie et al., 2015). Plaque isolated viruses were obtained by isolating individual viral plaques which were then amplified on BHK-21 cells. The baby hamster kidney BHK-21 fibroblast cell line (ATCC CCL-10) was used to grow viruses and to determine their titers. Viral titers for both viruses were determined by standard plaque assay on BHK-21 or SUIT-2 cells using an agar overlay, and then calculated as plaque-forming units (PFU) per ml or fluorescent focus units (FFUs) per ml. To calculate PFU/ml, cells were fixed and stained with crystal violet, whereas to calculate FFU/ml, VSV-encoded RFP fluorescent foci were counted using fluorescent microscopy. The following human PDAC cell lines were used in this study: SUIT-2 (Iwamura T et al., 1987), MIA PaCa-2 (ATCC CRL-1420), and AsPC-1 (ATCC CRL-1682). The human origin of all these PDAC cell lines was confirmed by partial sequencing of KRAS and actin, as well as genomic mutation profiling using Cancer Hotspot Panel v2 (Life Technologies) to analyze for 2800 Catalogue of Somatic Mutations in Cancer (COSMIC) mutations of 50 oncogenes and tumor suppressor genes (Hastie et al., 2016). As expected, all PDAC cell lines had a mutation in KRAS, as it is typical for PDACs (Cataldi et al., 2015; Hastie et al., 2016). A non-malignant human pancreatic duct epithelial (HPDE) cell line was previously generated by introduction of the E6 and E7 genes of human papillomavirus 16 into normal adult pancreas epithelium. HPDE

retains a genotype similar to pancreatic duct epithelium, is non-tumorigenic in nude mice, and has no cancer-associated mutations (Furukawa T et al., 1996). HPDE was grown in Keratinocyte-SFM (K-SFM, Gibco, 17005042) without serum. Normal untransformed human fibroblasts AG08498 and AG01519 from foreskin of healthy donors were obtained from Coriell Institute. MIA PaCa-2, SUIT-2 and AsPC-1cells were maintained in Dulbecco's modified Eagle's medium (DMEM, Cellgro, 10-013-CV), while BHK-21, AG08498 and AG01519 in modified Eagle's medium (MEM, Cellgro, 10-010-CV). All cell growth media (except for K-SFM that was supplemented with manufacturer-provided human recombinant Epidermal Growth Factor 1-53 (EGF 1-53) and Bovine Pituitary Extract (BPE)) were supplemented with 10% fetal bovine serum (FBS, Gibco), 4 mM L-glutamine, 900 units (U) per ml (U/ml) penicillin, 900 μg/ml streptomycin and 1% non-essential amino acids. MEM was additionally supplemented with 0.3% glucose (w/v). Cells were kept in a 5% CO_2 atmosphere at 37°C. For all experiments, all cell lines were passaged no more than 15 times.

3.1.2 Viral Passaging

MIA PaCa-2 and SUIT-2 cells were seeded into 35-mm dishes to be approximately 95% confluent in 24 h. Cells were washed once with PBS and incubated with viruses at an MOI of 0.1 PFU/ml (calculated based on virus titration on BHK-21) in DMEM without fetal bovine serum (FBS) for 1 h at 37°C. After the 1h incubation media containing unbound virus was aspirated, cells were washed with PBS, and fresh DMEM medium containing 5% FBS was added to the cells. After 24 h of incubation, dishes were checked under microscope (Olympus IX70 Fluorescence Microscope) to ensure all cells were infected, this was detected by the presence of RFP signal and that all cells were detached

from the 35-mm dishes. The entire supernatant was collected at 24 h p.i. and centrifuged at 4,000 rpm at 4°C for 10 min to pellet cellular material. The virus containing supernatant was transferred to new tubes and stored at -80°C. Each collected viral passage was used for the subsequent viral passage.

3.1.3 RNA isolation, cDNA generation, PCR amplification, and DNA sequence analysis

RNA was isolated from 100 µl of virus-containing supernatant using the Quick-RNA MiniPrep kit (Zymo Research, R1031 and R1033). 5 µl of total RNA per reverse transcription reaction and random hexamer primers were used with SMART-Scribe reverse transcriptase (Takara Bio, ST0065) to generate cDNA. PCR was done on the generated cDNA using VSV- or transgene- specific primers listed in Table 1 PCR products were electrophoresed on 1% agarose gels containing ethidium bromide in TBE buffer, PCR products were cut from the agarose gel from which DNA was extracted following DNA extraction kit protocol (Quiagen, #28706). DNA samples were then nanodropped and if DNA concentration was lower than 20 ng/µl, the sample was concentrated using a SpeedVac vacuum concentrator until a concentration of at least 20 ng/µl was obtained. In a microfuge tube, Following Eurofins Genomics instructions, DNA with a concentration between 20-60 ng/µl was combined with a single primer. The DNA and primer combinations were sent to Eurofins Genomics for Sanger sequencing. As per Eurofins Genomics sequencing algorithm, any base pair that obtained a Phred quality score of 20 or lower was marked as nonspecific (N). A Phred quality score of 20 or lower indicates a base call accuracy between 90-99%. All sequencing results were analyzed with SnapGene 4.3 software.

3.1.4 Viral replication kinetics assay and crystal violet cytotoxicity assay

For all experiments, multiplicity of infection (MOI) was determined by tittering viruses using standard plaque assays on BHK-21 cells in 24 well plates. For virus replication kinetics assays, cells were seeded in 96-well plates. Viral dilutions of all viruses were prepared in DMEM with 0% FBS and used to infect cells at MOI 0.1. Cells were washed once with PBS and virus was added to cells which were incubated at 37°C for 1 h. Virus containing media was aspirated and fresh DMEM with 5% FBS was added to cells that were further maintained at 37°C for the duration of the experiment. Virus-encoded RFP fluorescence levels were measured following incubation at 1, 21, 48, and 72 h p.i. using a fluorescence multiwell plate reader. RFP fluorescence was read at the wavelength 590/645 nm. For crystal violet cytotoxicity assay on multiple different cell lines, in a 96-well format, the first well was infected at MOI 0.15 (PFUs calculated based on virus titration on BHK-21), and then 6-fold serial dilutions were used to infect different cell lines. Each cell line was also mock treated (control). Cells were stained with crystal violet solution (2% crystal violet in methanol) at 72 h p.i. to detect cytotoxicity caused by viruses, and unstained wells represent those in which total cell lysis had occurred.

3.1.5 Western blot analysis

Cells were seeded into 12-well plates to be approximately 95% confluent after 24 h. Medium was removed and cells were washed once with PBS. Virus was then added at MOI 0.1 (calculated based on virus titration on BHK-21) in 0% FBS media and incubated for 1 h at 37°C. After the 1 h incubation, the virus containing media was removed and 5% FBS media was added to the cells. Cells were lysed and total protein was isolated 13 h p.i using buffer containing 0.0625 M Tris-HCl (pH 6.8), 10% glycerol, 2% SDS, 5% 2-

mercaptoethanol, and 0.02% (w/v) bromophenol blue. Total protein was separated by electrophoresis on 10% SDS-PAGE gels and electroblotted onto polyvinylidene difluoride (PVDF) membranes. Membranes were blocked by using 5% nonfat powdered milk in TBS-T (0.5 M NaCl, 20 mM Tris [pH 7.5], 0.1% Tween 20) overnight at 4°C or for 1 h at room temperature. Membranes were incubated with a 1:5,000 dilution of rabbit polyclonal anti-VSV antibodies (raised against VSV virions), a 1:1,000 dilution of rabbit anti-STAT1 total (Cell Signaling, 14994T, clone D1K9Y) or a 1:1,000 dilution of anti STAT1-phospho (Cell Signaling, D4A7), or a 1:5,000 dilution of anti-p53 (Cell Signaling, 1C12) in TBS-T with 5% milk with 0.02% sodium azide. For detection of horseradish peroxidase (HRP) conjugated secondary antibodies anti-Rabbit (Jackson ImmunoResearch, 111-035-003) and anti-mouse IgG (Jackson ImmunoResearch, 115-035-003). Amersham ECL Western Blotting Detection Kit was used. Alternatively, StarBright Blue 700 Goat Anti-Mouse (Bio-Rad, 12004158) and Anti-Rabbit IgG (Bio-Rad, 12004161) fluorescent secondary antibodies at 1:5,000 dilutions were used for fluorescent western blotting detection using ChemiDoc MP Imaging System from Bio-Rad. To verify total protein in each loaded sample the membranes were stained with Coomassie Blue.

3.1.6 Virion attachment assay

To assess VSV attachment to the cell monolayer, cells were seeded into a 12-well plate so that confluence was approximately 100% the next day. Medium was then removed, and cells were washed one time with PBS. Cells were place on ice approximately 5 minutes prior to virus infection to cool cells. Virus in DMEM (SUIT-2) or MEM (BHK-21) with 0% FBS was added to cells on ice, and cells were incubated for 1 h at 4°C. After incubation, virus containing media was aspirated and wells were washed 3 times with PBS to remove

any unbound virus. Samples then either had protein isolated immediately as previously described (to examine attachment) or were incubated for an additional 7 h at 37°C (to examine VSV replication) and then had total protein isolated. Total protein was analyzed by western blot as described above. Membranes were initially blocked in 5% non-fat milk in TBS-T. Membranes were then incubated with a 1:5,000 dilution of rabbit polyclonal anti-VSV antibodies (raised against VSV virions) in TBS-T with 5% milk followed by a 1:10,000 dilution of anti-rabbit secondary antibodies. To verify total protein in each sample loaded membranes were stained with Coomassie Blue.

3.1.7 Virus Purification

To grow and purify VSV, BHK-21 cells were infected with at an MOI of 0.01 and incubated at 37°C in MEM 5% FBS. Virus containing media was collected around 48 h p.i. The media was centrifuged at 4,000 × g for 10 min using the Eppendorf 5810R centrifuge to remove large cellular debris. The supernatants were underlaid with 5 ml 20% (w/v) sucrose in HEN buffer (10 mM HEPES pH 7.4, 1 mM EDTA, 100 mM NaCl) and centrifuged at 28,000 rpm and 4°C for 3.5 h in a Beckman SW32 Ti rotor. The virus-containing pellet was resuspended overnight in HEPES buffered saline, pH 7.5 [HBS; 21 mM HEPES, 140 mM NaCl, 45 mM KCl, 0.75 mM Na_2HPO_4, 0.1% (w/v) dextrose] and then centrifuged in a 7.5–27.5% continuous gradient of Optiprep (Axis Shield) in HBS at 26,500 rpm and 4°C for 30 min using a Beckman SW40 Ti rotor. The viral band was removed from the gradient, diluted with ET buffer (1 mM Tris-HCl pH 7.5, 1 mM EDTA), pelleted by centrifugation at 27,000 rpm and 4°C for 1.5 h using a Beckman SW40 Ti rotor and resuspended in ET buffer.

3.1.8 Inhibition of VSV infection with soluble LDLR

To analyze the effect of sLDLR on VSV, Single Mutant E238K, and Double Mutant E238K and K174E, cells were seeded into 12-well plates so that they were 95% confluent after 24 h. MOI 0.1 virus dilution without sLDLR and MOI 0.1 virus dilution with 1 μg/mL of sLDLR (catalog number 2148-LD-025; R&D Systems) were incubated for 30 min at 37°C. Medium was aspirated from cells which were then washed once with PBS. Virus dilutions incubated with or without sLDLR for 30 min were added to cells and incubated for 30 min at 37°C. After the 30 min incubation, the media used for infection was aspirated and cells were washed once with PBS. Fresh DMEM containing 5% FBS was added to cells. 13 h p.i RFP containing cells were counted using a Nexcelom Vision Image Cytometer to determine the percentage of RFP infected cells. The percent of virus-infected cells was calculated by dividing the number of RFP-positive cells by the total number of cells counted.

3.1.9 Effects of DEAE-Dextran on VSV p53wt (Founder) and VSV-p53wt (SUIT-2) infectivity and replication

BHK-21, SUIT-2 and MIA PaCa-2 cells were seeded into a 96-well plate to be approximately 100% confluent at the time of treatment and infection. Cells were washed once with PBS containing Mg^{2+} and Ca^{2+}. Prior to infection, cells were pretreated with MEM without FBS (mock) or with 10 μg/ml DEAE-dextran in MEM without FBS for 30 min. After the 30 min pretreatment, VSV p53wt (Founder) or VSV-p53wt (SUIT-2) in MEM with 0% FBS was directly added to cells at an MOI of either 1, 0.1 or 0.01 (MOI calculated based on virus titration on BHK-21) for 1 h at 37°C. Virus + DEAE-dextran containing media was removed after the 1 h infection period and fresh DMEM containing 5% FBS was added to cells. Cells were maintained at 37°C and the level of VSV-encoded

RFP fluorescence was measured over the course of 68 h p.i using a fluorescence multiwell plate reader at the wavelength 590/645 nm.

3.2 Results

3.2.1 Experimental evolution of two oncolytic VSV variants in two human PDAC cell lines

For each passage, fresh uninfected cells were infected at an MOI of 0.1 plaque forming units (PFU) per ml (calculated based on titrating viruses on BHK-21 cells) by incubating fresh cells for 1 hour (h) with a previous virus passage, washing off any unbound virus, and incubating cells for an additional 23 h. Supernatant from the infected cells was collected 24 h post infection (p.i.) to be used for the next passage while the remaining supernatant was saved and stored at -80°C. After a final passage ("Passage 32") on a PDAC cell line, each virus was amplified on BHK-21 to generate the following four "Passage 33" viruses: VSV-p53wt (MIA PaCa-2), VSV-p53-CC (MIA PaCa-2), VSV-p53wt (SUIT-2), and VSV-p53-CC (SUIT-2). This final amplification on BHK-21 was done to generate stocks of virus particles comparable to the founder virus particles which were originally amplified on BHK-21 cells (Fig. 2A).

3.2.2 Viral genome sequence analysis of passaged viruses

To examine if any mutations within coding (viral or transgenic) or non-coding regions of viral genomes took place over the course of the 33 passages, genomes of each founder virus and passage 33 virus were fully sequenced using Sanger sequencing. Despite the advantages of next-generation sequencing techniques, Sanger sequencing allowed us to focus on major advantageous mutations that would become fixed or at least highly prevalent in viral populations by passage 33. For sequencing, supernatants containing viral particles were used to isolate viral genomic RNA that was reversed transcribed into cDNA

using random hexamer primers. The generated cDNA was then PCR amplified to generate overlapping DNA products covering the entire viral genomes using primers described in Table 1.

Figure 3C summarizes all genome alterations in viruses detected by Sanger sequencing. No mutations were detected in the VSV regions N, M, p53, RFP, or any intergenic regions of viral genome. The absence of any novel mutations in VSV-M after 33 passages is particularly important, indicating the stability of in M-ΔM51 as an oncolytic virus attenuator. Of the passage 33 viruses that were passaged on the cell line MIA PaCa-2, one missense mutation E860D, only partially present in passage 33 viral population (data not shown), was detected in the L protein coding region of VSV-p53wt (MIA PaCa-2). This mutation was not present in any other virus. As we expected, SUIT-2 passaged viruses acquired more mutations than the MIA PaCa-2 passaged viruses, likely because of the stronger selective pressure in SUIT-2 cells. VSV-p53wt (SUIT-2) had a total of 3 nt substitutions: 2 missense mutations in VSV-G and one silent mutation in VSV-L. VSV-p53-CC (SUIT-2) had a total of 5 nt substitutions: 3 missense mutations in VSV-G, 1 silent in VSV-P, and 1 silent in VSV-L (Fig. 3C).

3.2.3 Stability of transgenes over extensive viral passaging

To examine the stability of VSV-encoded transgenes, we amplified and sequenced a portion of viral genome containing transgene sequences between VSV-G and VSV-L coding regions (Fig. 3A). As controls, we used a plasmid containing a full-length cDNA copy of the viral genome of VSV-p53wt ("VSV-p53wt plasmid" in Fig. 3A), and cDNA generated from a VSV-eq-FP650 virus that encodes a shorter transgene (RFP only, no p53 sequences) ("VSV-eq-FP650" in Fig. 3A). If passaged viruses lost any significant portions

of their transgenes, we expected to see shorter PCR fragments. In addition, all these PCR fragments were sequenced to detect any nt changes in this region. We did not detect any deletions in the transgene regions in any of the passage 33 viruses (Fig. 3A). Moreover, we detected no nt deletions, additions or substitutions in the transgenes by Sanger sequencing. To independently address the issue of potential transgene loss, we also examined virus titers for founder and passage 33 viruses by comparing plaque forming units (PFUs) and fluorescent focus units (FFUs). PFUs would account for all infectious viruses (with and without RFP expression), while FFUs would account only for viruses retaining their transgene. We did not observe any significant changes in the FFU/PFU ratios for founder and passage 33 viruses indicating that the passage 33 viruses have not lost RFP transgene sequences (Fig. 3B). Together, our data demonstrates long-term stability of VSV-encoded RFP-p53 transgenes after extended replication of tested viruses in either permissive or moderately resistant PDAC cell lines.

3.2.4 Identification of 2 identical mutations in suit-2 passaged viruses

Surprisingly, both of the SUIT-2 passaged viruses acquired 2 identical missense mutations in VSV-G at aa positions 238 (G→A nt substitution) and 174 (A→G nt substitution): E238K and K174E (Fig. 3C). To see at what point these mutations occurred during viral passaging, we sequenced VSV-G of each virus at intermittent passages. Figure 3 shows that in both VSV-p53wt (SUIT-2) and VSV-p53-CC (SUIT-2), E238K appeared first around passage 10, followed by K174E that first appeared around passage 26 in VSV-p53wt (SUIT-2) and passage 27 in VSV-p53-CC (SUIT-2). Interestingly, only after K174E became dominant in both viruses (around passage 30), E238K quickly reached fixation (complete sweep) (Fig. 4). Also, while the E238K mutation was slowly replacing the WT

position between passage 10 and 33, the K174E reached fixation (complete sweep) surprisingly quickly, just in several passages after appearing first around passage 27.

3.2.5 Identification of a third mutation in VSV-P53-CC (SUIT-2)

Compared to VSV-p53wt (SUIT-2), VSV-p53-CC (SUIT-2) obtained another mutation in VSV-G, M184I (G→A nt substitution) (Fig. 3C and Fig. 5). Although M184I has never completely replaced the WT position in the viral population of passage 33 VSV-p53-CC (SUIT-2), it was fixing in the population surprisingly quickly, first appearing at passage 28 and becoming prevalent by passage 33 (Fig. 5).

3.2.6 SUIT-2 passaged viruses show an improved replication in PDAC cells, while retaining their oncoselectivity

To determine whether the mutations in passaged viruses altered VSV abilities to replicate in PDAC or nonmalignant cells, virus replication kinetic assays were conducted to compare the founder viruses to the passage 33 viruses. In addition to MIA PaCa-2 and SUIT-2, we tested another human PDAC cell line, AsPC-1, which has a similar phenotype to SUIT-2 in terms of the permissiveness to VSV (moderately resistant) and antiviral status (inducible type I IFN signaling) (Hastie et al., 2015; Moerdyk-Schauwecker et al., 2013). We also tested the viruses in BHK-21, which are highly permissive to VSV and many other viruses at least in part due to their defective antiviral responses (Habjan et al., 2008; Otsuki et al., 1979). To examine the possible loss of oncoselectivity of the passaged viruses as a result of the acquired mutations, we also compared the viruses in the nonmalignant human pancreatic duct epithelial cell line HPDE (Furukawa T et al., 1996) and the primary human fibroblast cell lines AG0159 and AG08498.

To examine VSV replication kinetics, the founder and passage 33 viruses were first titrated on BHK-21. Based on the determined virus titers on BHK-21, different cell lines

were infected at MOI 0.1, and VSV-encoded RFP fluorescence was measured at 1, 21, 48, and 72 h p.i. (Fig. 6). As shown in previous studies, due to its downstream position between VSV-G and VSV-L, virus-encoded reporter expression can be used to measure virus replication levels as it could be detected only if the virus genome is replicated (Boritz et al., 1999). The experiment showed that while all tested viruses showed similar levels of replication in BHK-21 and MIA PaCa-2, both VSV-p53wt (SUIT-2) and VSV-p53-CC (SUIT-2) replicated better in SUIT-2, compared to founder viruses, especially at 21 h p.i. Importantly, both VSV-p53wt (SUIT-2) and VSV-p53-CC (SUIT-2) replicated better not only in SUIT-2, but also in AsPC-1 cells, and they retained the abilities of founder viruses to replicate in MIA PaCa-2 cells, indicating that experimental evolution of viruses in SUIT-2 cells widened the range of PDAC cells permissive to VSV.

While SUIT-2-passaged viruses show an improved ability to replicate in SUIT-2 and AsPC-1 cell lines, they also show a retention of oncoselectivity, as none of the tested viruses showed detectable replication in HPDE or either of the tested primary human fibroblast cell lines (Fig. 6). In agreement with virus replication kinetics assay (Fig. 6), crystal violet cell cytotoxicity assay showed an improved cell killing for SUIT-2-passaged viruses in SUIT-2 cells, but no cell killing in HPDE cells (Fig.7).

3.2.7 K174E is required for an improved replication of VSV experimentally evolved in SUIT-2 cells

As both VSV-p53wt (SUIT-2) and VSV-p53-CC (SUIT-2) obtained the same 2 mutations in VSV-G (first E238K, then later K174E) (Fig. 3 and 4), we next determine whether E238K alone or both mutations were required for the observed similar phenotypes of these SUIT-2-passaged viruses. To address this question, SUIT-2 passage 20 of VSV-p53wt (to isolate viruses with no mutations or only E238K) and SUIT-2 passage 33 of

VSV-p53wt (to isolate viruses with both E238K and K174E mutations) were serially diluted until only 1 FFU was microscopically observed in a tissue culture well, then each virus originated from a single FFU was amplified in BHK-21 cells, and viral genome was sequenced to verify VSV-G sequence. Using this approach, we obtained 12 independent VSV-p53wt based viruses each originated from a single FFU (hereinafter referred to as "independent virus clones"), 4 with no mutations in G ("WT VSV-G"), 4 with E238K only mutation ("Single Mutant"), and 4 with both E238K and K174E mutations ("Double Mutant") (Fig.8). No virus clones with only the K174E mutation were evaluated in this study as that mutation was only present together with the E238K mutation. Based on the determined virus titers on BHK-21, BHK-21 and SUIT-2 cells were infected at MOI 0.1, and replication of these "independent virus clones" was examined by western blot by analyzing accumulation of viral proteins at 8, 13, 18 and 24 h p.i. As shown in Figure 8, no detectable stimulation of viral replication was observed for any of the 4 Single Mutants (G-E238K) in either BHK-21 or SUIT-2 cells, while clear improvement in viral replication can be seen for all Double Mutants at all tested time points in SUIT-2 cells and at earlier time points (especially at 8 h p.i.) in BHK-21 cells. These data indicate that the second mutation K174E was required for improved replication of VSV experimentally evolved in SUIT-2 cells.

3.2.8 Acquired G mutations do not inhibit antiviral signaling and retain oncoselectivity

SUIT-2 cells are able to induce a functional type I IFN response to VSV (Bressy et al., 2019; Hastie et al., 2015; Moerdyk-Schauwecker et al., 2013). Therefore, we hypothesized that extensive passaging of VSV on SUIT-2 cells selected for spontaneous VSV mutants via an improved ability to evade type I IFN signaling. If this hypothesis is

correct, we would expect to see an increase in VSV replication accompanied by a decrease in antiviral signaling when SUIT-2 cells are infected with the evolved viruses. To test this hypothesis, we infected SUIT-2 and other cell lines shown in Figure 9 with different viruses at MOI 0.1 (calculated based on titration of viruses on BHK-21 cells), total protein was isolated at 13 h p.i. and analyzed by Western blotting for accumulation of VSV-encoded proteins as well as total STAT1 and phosphorylated STAT1 (STAT1-P) levels as a marker of type I IFN signaling induction (Fig. 9). In agreement with our data in Figures 6-8, VSV-p53wt (SUIT-2) and VSV-p53-CC (SUIT-2) showed an increased ability to replicate on SUIT-2 cells (Fig. 9). Interestingly, these 2 viruses also showed a slightly increased ability to replicate in MIA PaCa-2 cells, which are defective in type I IFN signaling. We did not detect significant differences in viral replication levels in BHK-21 cells at 13 h p.i., which is consistent with the data shown in Figure 8, where the differences in BHK-21 cells were seen only at an earlier time point (8 h p.i.). No significant viral replication was detected in the non-malignant pancreatic ductal cell line HPDE and human primary fibroblast cell lines AG0159 and AG08498, confirming retained oncoselectivity of the evolved viruses (Fig. 8). Importantly, although viral infections did not significantly alter total STAT-1 levels, for both of the SUIT-2 passaged viruses in SUIT-2, HPDE, and both of the fibroblast cell lines there was an increase, rather than decrease, in STAT1 phosphorylation in VSV-p53-CC (SUIT-2) and VSV-p53wt (SUIT-2) infected cells (Fig. 9). In general, our data show no inhibition of antiviral signaling by VSV-p53-CC (SUIT-2) and VSV-p53wt (SUIT-2) viruses.

When a similar experiment was conducted with the independent virus clones of VSV-p53wt (WT G, Single Mutant G, and Double Mutant G mutants), the same

improvement in viral replication in SUIT-2 cells at 13 h p.i. required the second VSV-G mutation K174E (Fig.10). As in Fig. 9, we did not see significant differences in viral replication in MIA PaCa-2 or BHK-21 cells at 13 h p.i. and, importantly, no increased viral replication in the primary fibroblast cell line AG01519 indicating retained oncoselectivity of both the Single and Double Mutant viruses. This experiment also included VSV-p53wt (Founder) ("P0" in Fig. 9) and VSV-p53wt (SUIT-2) ("P33" in Fig. 10) viruses, and VSV-p53wt (SUIT-2) was very similar to independent virus clones of VSV-G Double Mutants.

3.2.9 Acquired G mutations improve attachment to SUIT-2 cells

Since both VSV-p53-CC (SUIT-2) and VSV-p53wt (SUIT-2) mutations were located in VSV-G, a region that plays an important role in viral attachment, and because our previous studies have shown that VSV does not attach to SUIT-2 cells as well as to some other PDAC cell lines (Felt et al., 2017), we also compared the ability of the founder and SUIT-2-passaged viruses to attach to SUIT-2 cells. To examine virus attachment, BHK-21 or SUIT-2 cells were incubated at various MOIs (calculated based on titration of viruses on BHK-21 cells) with purified VSV-p53wt (Founder) or VSV-p53wt (SUIT-2) at 4°C for 1 h, cells were extensively washed to remove any unbound virus and analyzed by western blot for virus proteins bound to cells ("Attachment" assay in Fig. 11A). At 4°C, the viral particles can only attach to the outside of cells and not enter them. A duplicate set of cells was treated the same way (incubation with virus at 4°C for 1h, then extensively washed), but then incubated for 7 more h at 37°C before protein was isolated to examine virus replication ("Replication" assay in Fig. 11A). Only the VSV-p53wt viruses were used in this assay to examine the role of the 2 mutations shared between the VSV-p53wt and VSV-p53-CC viruses. In BHK-21, there was only a minor difference in virus attachment

or replication between VSV-p53wt (Founder) or VSV-p53wt (SUIT-2) viruses. In SUIT-2 cells, VSV-p53wt (SUIT-2) was able to attach much more efficiently (about 3-fold better based on serial dilutions of viruses) than VSV-p53wt (Founder), and VSV-p53wt (SUIT-2) replication of the passage 33 virus was also higher on SUIT-2 cells. These data suggest that the SUIT-2-passaged viruses were selected to attach to SUIT-2 cells more efficiently, that could improve new infection efficacy and explain at least in part the observed improvement in viral replication of SUIT-2-passaged viruses. To test whether SUIT-2-passaged viruses could initiate infections more efficiently, compared to founder viruses, serial dilutions of each virus were titered on BHK-21 and SUIT-2 cells, and the ratios of virus titers on SUIT-2 cells to BHK-21 cells were calculated. As shown in Fig. 11B, VSV-p53wt (SUIT-2) and VSV-p53-CC (SUIT-2) improved their abilities to initiate infections on SUIT-2 cells by about 3-fold, which is consistent with our data on relative attachment efficiency of founder and passaged viruses (Fig. 11A).

3.2.10 SUIT-2 adapted viruses are still able to interact with LDLR

LDLR and LDLR family members have been shown to serve as receptors for VSV (Amirache et al., 2014; Ammayappan et al., 2013; Finkelshtein et al., 2013; Nikolic et al., 2018). As VSV-G is responsible for VSV attachment to host cells and we observed an improved attachment of SUIT-2-passaged viruses to SUIT-2 cells (Fig. 11A), we wanted to examine the abilities of evolved viruses to attach to LDLR. Mutations in VSV-G could improve VSVs ability to interact with LDLR or, rather, utilize an alternative receptor. To determine if VSV mutants are still able to interact with LDLR and to the same degree as WT VSV, the affinity of VSV for LDLR was examined using soluble LDLR (sLDLR) that neutralizes VSV virions and inhibits viral infectivity. To test if sLDLR could inhibit

independent "virus clones" (WT-G, Single Mutant, or Double Mutant) of VSV-p53wt (the same number of infectious particles corresponding to an MOI 0.1 infection on BHK-21 cells were used) were incubated with or without sLDLR *in situ*, and then SUIT-2 cells were incubated with these VSV+/-sLDLR combinations for an additional 30 min, then washed to remove any unattached virus and sLDLR, and incubated for an additional 12 h. Cells were then trypsinized and analyzed for the percentage of VSV-infected cells (RFP-positive cells). In agreement with Figure 8 data, the presence of both VSV-G mutations, E238K and K174E, in Double Mutants resulted in a dramatic increase in the percentage of VSV-infected cells in the presence or absence of sLDLR (Fig. 12A and Fig. 12B). However, we did not observe statistically-significant differences between viruses in regard to the inhibiting effect of sLDLR on viral infectivity (Fig. 12C). These data suggest that VSV is still able to attach to and infect SUIT-2 cells through an interaction with LDLR.

3.2.11 Treatment with DEAE-dextran does not improve SUIT-2 adapted viruses replication in SUIT-2 cells

We have previously shown that infectivity of VSV-ΔM51 in several resistant PDAC cell lines, including SUIT-2, was dramatically improved when cells were treated with the polycations DEAE-dextran or polybrene (Felt et al., 2017). Although the exact mechanism of polycation-mediated improvement of virion attachment is not clear and several alternative mechanisms, including charge shielding and virus aggregation, have been proposed (Davis et al., 2004), it is believed that polycations facilitate the initial non-specific anchoring of virus particles to cell surface, which facilitates their further association with specific receptors (such as LDLR and LDLR family members for VSV) (Denning et al., 2013; Pizzato et al., 1999; Reiser et al., 1996; Sharma et al., 2000; Yee et al., 1994). As our data suggest that the VSV-G mutations E238K and K174E did not

dramatically change VSV-G affinity for LDLR, we decided to test a hypothesis that E238K and K174E mutations improve the efficacy of this initial non-specific VSV binding to target cells. In such case, the efficient infection of evolved viruses would be less dependent on polycation treatment, compared to the founder viruses. To test this hypothesis, we infected BHK-21, MIA PaCa-2, and SUIT-2 with the founder viruses and the SUIT-2-passaged viruses at various MOIs (calculated based on titration of viruses on BHK-21 cells) in the presence or absence of DEAE-dextran, and analyzed virus replication kinetics by measuring VSV-encoded RFP fluorescence over time. In agreement with our previous study using VSV-ΔM51 (Felt et al., 2017), we did not observe any significant positive effect of DEAE-dextran on replication of any tested viruses in highly permissive BHK-21 and MIA PaCa-2 cell lines (Fig. 13). On the other hand, in agreement with the same study (Felt et al., 2017), DEAE-dextran treatment strongly improved infectivity of VSV-p53 (Founder) at all tested MOIs in SUIT-2 cells (Fig. 13). In contrast, DEAE-dextran treatment had a rather small positive effect on VSV-p53 (SUIT-2) infection only at the lowest MOI tested (MOI 0.01), and no effect was observed at MOI 0.1. Moreover, DEAE-dextran treatment actually inhibited VSV-p53 (SUIT-2) at MOI 1 (Fig. 13). In general, these data indicate that VSV G mutations K174E and E238K make the evolved viruses less dependent on polycations for efficient infection of resistant cell lines, such as SUIT-2, suggesting that the evolved viruses have an improved nonspecific attachment to target cells.

3.2.12 E238K and K174E location analysis in pre and post-fusion states

The location of VSV-G E238K and K174E mutations on crystallographic structures of pre-fusion and post-fusion states of the glycoprotein G were analyzed. The exact

location of the mutated residues within the VSV-G peptide sequence are located in figure 14. While no obvious alterations in interactions with VSVs known receptor, LDLR are apparent, E238 is surrounded by positively charged residues. Both E238 and K174 are positioned away from the binding region of VSV-G and LDLR CR2 region. Representation of low-pH, post-fusion conformation of VSV-G trimer (left) and VSV-G monomer (right) (Fig.15B). Both E238 and K174 are positioned away from the intermonomer interface in the protein VSV-G trimer (left). Histidine H226 is sandwiched by E238 and K174 (right). The E238K and K174E mutations are located near the region that undergoes the major conformational rearrangement during the transition from prefusion to postfusion state. They are about 24 Å apart in the prefusion conformation, but only about 10 Å apart in the postfusion conformation. Interestingly, in all passages, we found that the E238K mutation occurs first and the K174E mutation occurs within several passages after. E238 is located on the central beta-strand of the DIII (pleckstrin homology, PH) domain and is surrounded by positively charged residues including K44, K220, K225, H226, and K242 (Figure 15). The substitution of E238 for lysine would disturb the balance of positive and negative charge in this region, which could potentially lead to a conformational rearrangement. Furthermore, in a postfusion conformation, a histidine residue H226 is positioned between E238 and K174 residues, with the distance of 4 Å and 7 Å between the sidechains of H226 and of E238 and K174, respectively. Therefore, it is plausible to assume that the K174 mutation is a “rescue” mutation that re-establishes the balance of positive and negative charge around the histidine, which could be important for the conformational transition from prefusion to postfusion state.

3.3 Figures and Tables

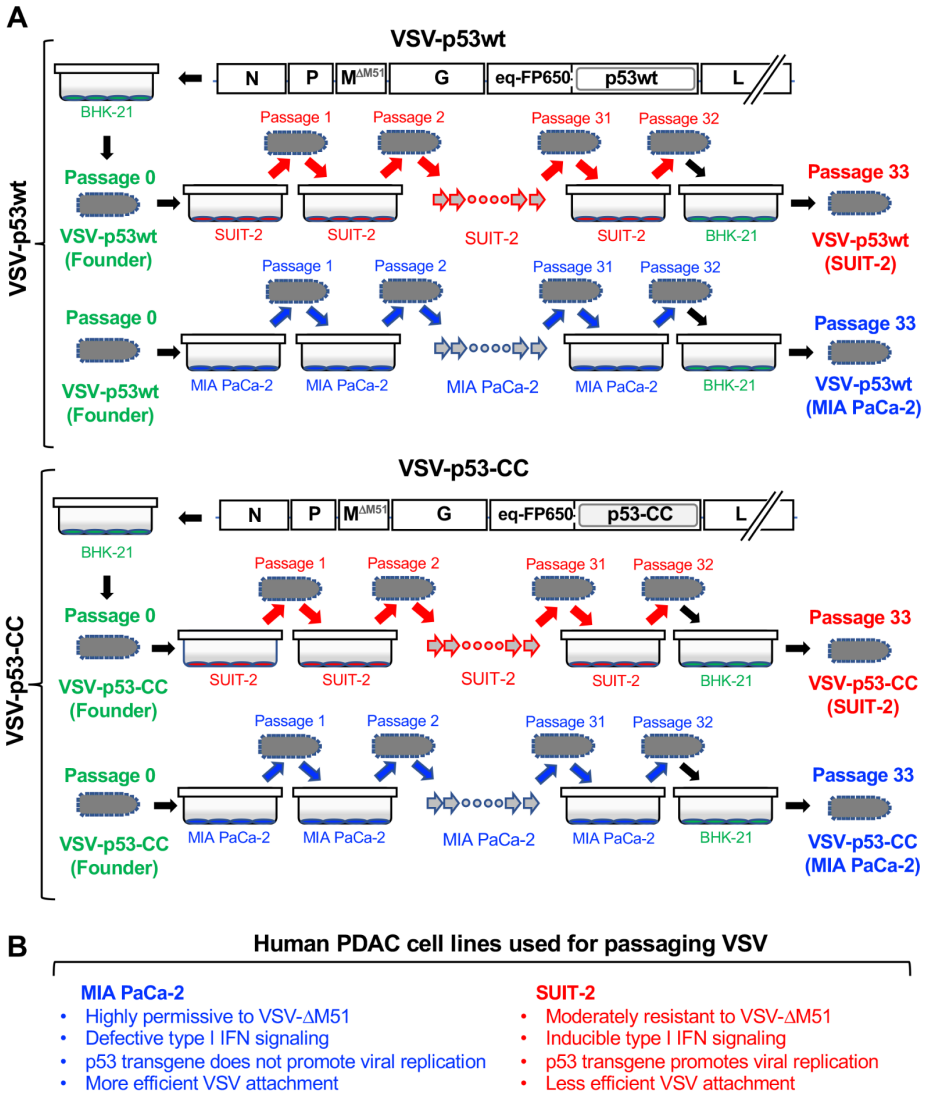

Figure 2. Scheme of viral passaging**.**

(A) Viruses VSV-p53wt (Founder) and VSV-p53-CC (Founder) ("Passage 0", amplified in BHK-21 cells) were serial passaged independently 32 times on the PDAC cell lines MIA PaCa-2 or SUIT-2. VSV-p53wt (Founder) and VSV-p53-CC (Founder) was added at an MOI of 0.1 (MOI calculated based on virus titration on BHK-21) to fresh cells for each

passage. Cells were incubated with virus for 1 h after which the virus was removed and fresh media was added. Virus containing supernatant was collected 24 h p.i., which was used for each subsequent viral passage (MOI of 0.1 infection). Each virus had a final passage on BHK-21 cells resulting in the following Passage 33 viruses used throughout this study: VSV-p53wt (MIA PaCa-2), VSV-p53-CC (MIA PaCa-2), VSV-p53wt (SUIT-2), and VSV-p53-CC (SUIT-2). (B) Characteristics of PDAC cell lines used in viral passaging, MIA PaCa-2 and SUIT-2. The information is based on the previously published studies (Bressy et al., 2019; Hastie et al., 2015; Moerdyk-Schauwecker et al., 2013).

Table 1: Primers used for VSV PCR amplification and sequencing.

N/A - not applicable

PCR Product No.	(+) Primer	(-) Primer	Expected PCR size	Region Amplified
1	VG380: acgaagacaaacaaaccattattatcat	VG381: caacaaacctgctgtagtaagag	1062	Genome end to N
2	VG72: ccctgccttccacttctg	VG75: tgggttggaaagtcatggat	1079	N to P
3	VG74: cgattaaagcagtcgtgcaa	VG382: agaagggacgtttccctgcc	743	P to M
4	VG31: cccaatccattcatcatgagttcc	VG32: cacttcatagtgacgcgtaaacag	848	M
5	VG383: gagagaaggccttaatgtttggcc	VG384: cctgaattagacttacatccactgagg	1092	M to G
6	VG385: agactcccatcaggtgtctggtt	VG386: gtggtggccgttcacggtgccc	932	G to eqFP650
7	VG245: ctccgagttggtatccatctttgc	VG387: gggacggcaaggggacagaac	966	G to p53
8	VG294: ggaaagaatcaaggaggcc	VG388: gccaacctcaggcggctcataggg	781	eqFP650 to p53
9	VG294: ggaaagaatcaaggaggcc	VG246: caagtacgtcatgcgctcatcggg	1522	eqFP650 to L
10	VG245: ctccgagttggtatccatctttgc	VG246: caagtacgtcatgcgctcatcggg	2273	G to L
11	VG389: ccaaatcaacttgtgataccatgctc	VG390: gtcttgctctgagaacaggttgtc	864	L
12	VG391: gaaacttgatattctaatggaccg	VG392: cgatgggtctagtaagtcgggta	727	L
13	VG393: tggagataaatggcatgaacttcc	VG394: aagtcctaacttccctgtccct	961	L
14	VG395: ggtgctctcaatcaaatggtttc	VG396: cccgtgaactaaagacgtcatg	1237	L
15	VG397: gaaaagagactccttgtgcaccatg	VG398: gggaatcgtttctaattcgtctc	1055	L
16	VG399: cagtgtacggaggtttgatttacttg	VG400: gccccaagcctgctttgagtcg	969	L
17	VG401: ctcctgagccccccagtgccct	VG402: gttcggaggtatcggtcctactc	746	L
18	VG403: gcggctgccttaaaatcatctgat	VG404: acgaagaccacaaaaccagat	687	L to genome end
N/A	VG405: ggaattggtccgaaaccaagttcg		N/A	Used to sequence PCR Product 1, in addition to VG 380 and VG381
N/A	VG406: cggatgtcctttaatgctccatac		N/A	Used to sequence PCR Product 18, in addition to VG 403 and VG404

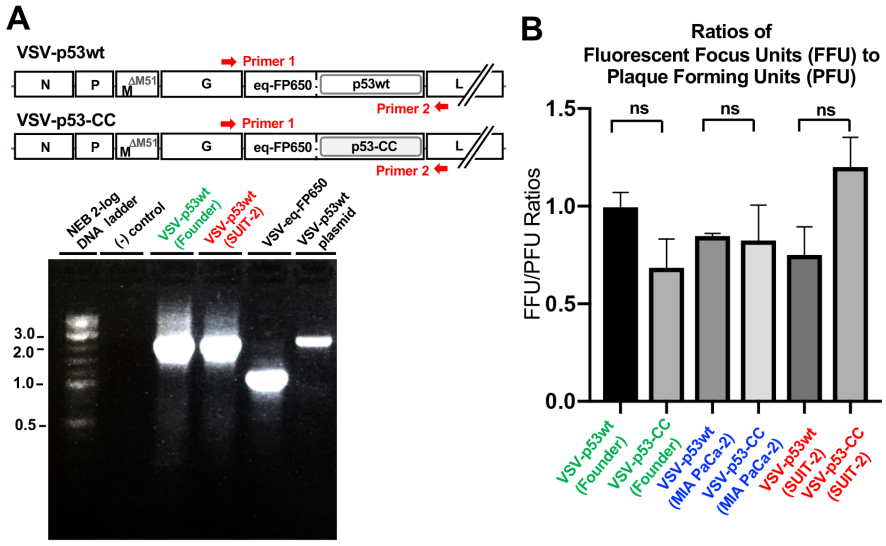

C "ND" – mutations not detected

Virus	N	P	M (ΔM51)	G	Eq-FP650	p53	L	Non-coding regions
VSV-p53wt (Founder)	ND	ND	ND	ND	ND	ND	ND	ND
VSV-p53-CC (Founder)	ND	ND	ND	ND	ND	ND	ND	ND
VSV-p53wt (MIA PaCa-2)	ND	ND	ND	ND	ND	ND	E860D (a9268c)	ND
VSV-p53-CC (MIA PaCa-2)	ND	ND	ND	ND	ND	ND	ND	ND
VSV-p53wt (SUIT-2)	ND	ND	ND	K174E (a3642g) E238K (g3834a)	ND	ND	V621V (g8551a)	ND
VSV-p53-CC (SUIT-2)	ND	L113L (t1734c)	ND	K174E (a3642g) E238K (g3834a) M184I (g3674a)	ND	ND	R55R (g6853a)	ND

Figure 3. Examination of transgene stability and sequencing of viral genomes.

(A) Analysis of transgene containing sequence between VSV-G and VSV-L to examine the stability of VSV-encoded transgenes. Supernatants containing viral particles for the founder and passaged viruses were used to isolate viral genomic RNA that was reversed

transcribed into cDNA using random hexamers. This cDNA was then amplified by PCR using primers described in Table 1. Red arrows show an approximate position of annealing sites for VSV specific primers (described in Table 1) located in VSV-G and VSV-L regions. As controls, we used a plasmid containing full-length copy of viral genome of VSV-p53wt and cDNA generated from VSV-eq-FP650 virus that encodes a shorter transgene (RFP only, no p53 sequences). (B) Comparison of the ratios of viral titers calculated by FFUs divided by PFUs indicates no loss of RFP transgene sequences from the viral genome after 33 passages. Results shown are representative of 2 independent repeats. Data shown represent the means and SEM of the means. Results were analyzed to determine significance using One-way ANOVA with a Tukey posttest at a 95% confidence interval for comparison between each condition, all conditions tested were statistically insignificant with no p-value < 0.05. (C) The entire genomes for all founder and passage 33 viruses were sequenced using Sanger sequencing. Supernatants containing viral particles for the founder and passaged viruses were used to isolate viral genomic RNA that was reversed transcribed into cDNA using random hexamers. This cDNA was then amplified by PCR using primers described in Table 1. All identified mutations are listed in the table above. Silent mutations are denoted in black font whereas missense mutations are denoted in bolded black font and highlighted in grey if only present in one virus or highlighted in yellow if present in two viruses. The region of the viral genome where the mutations were identified is located at the top of the table. “NM” – no mutations found.

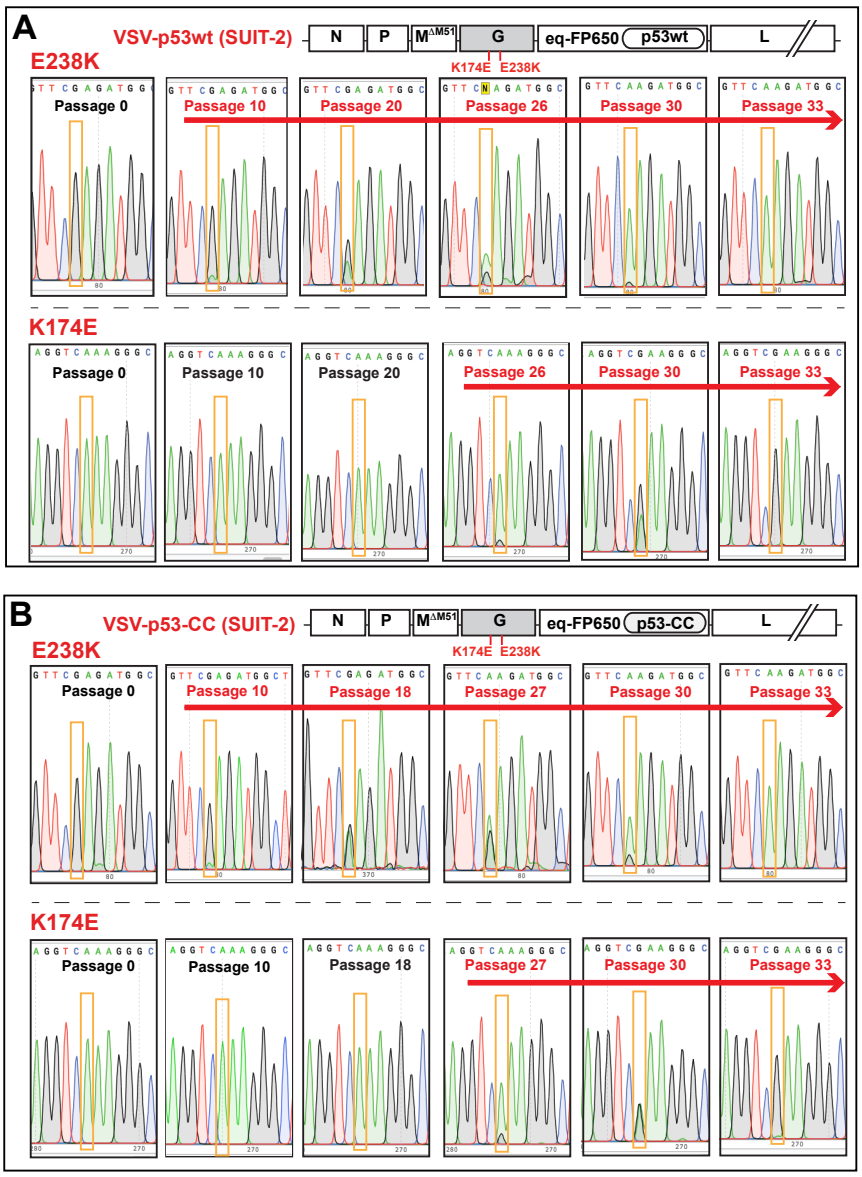

Figure 4. The chronological order of the appearance of VSV-G mutations E238K and K174E during passaging of viruses on SUIT-2 cells.

Supernatants containing viral particles for the shown passages were used to isolate viral genomic RNA that was reversed transcribed into cDNA using random hexamers. cDNA was PCR amplified using the primers VG383 and VG384 (described in Table 1) and the VSV-G regions containing aa positions 238 and 174 were sequenced with the same

primers. The nucleotide substitutions are highlighted in orange boxes and the presence of either mutation is indicated by a red arrow above the sequences.

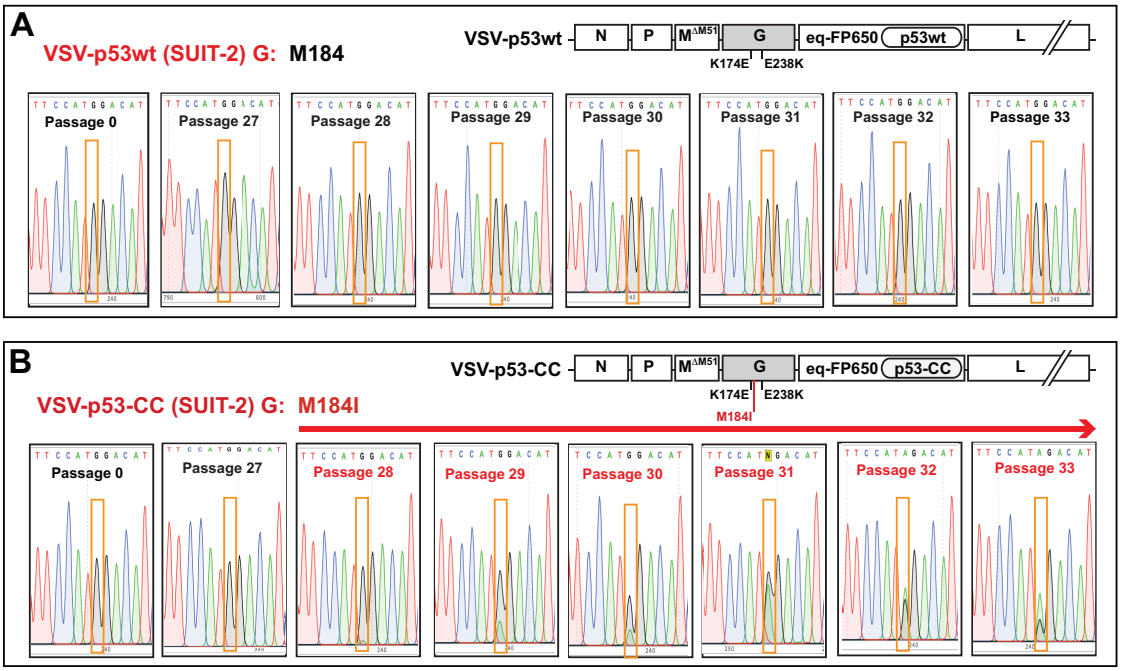

Figure 5. Chronological appearance of M184I mutation in VSV-p53-CC (SUIT-2).

The chronological order of the appearance of VSV-G mutation M184I, which was found in VSV-p53-CC (SUIT-2), but not in VSV-p53wt (SUIT-2). Supernatants containing viral particles for the shown passages were used to isolate viral genomic RNA that was reversed transcribed into cDNA using random hexamers. This cDNA was PCR amplified using the primers VG383 and VG384 (described in Table 1) and the VSV-G region containing aa position 200 was sequenced using primers VG383 and VG384. The nucleotide substitutions are highlighted in orange boxes and the presence of M184I mutation is indicated by a red arrow above the sequences.

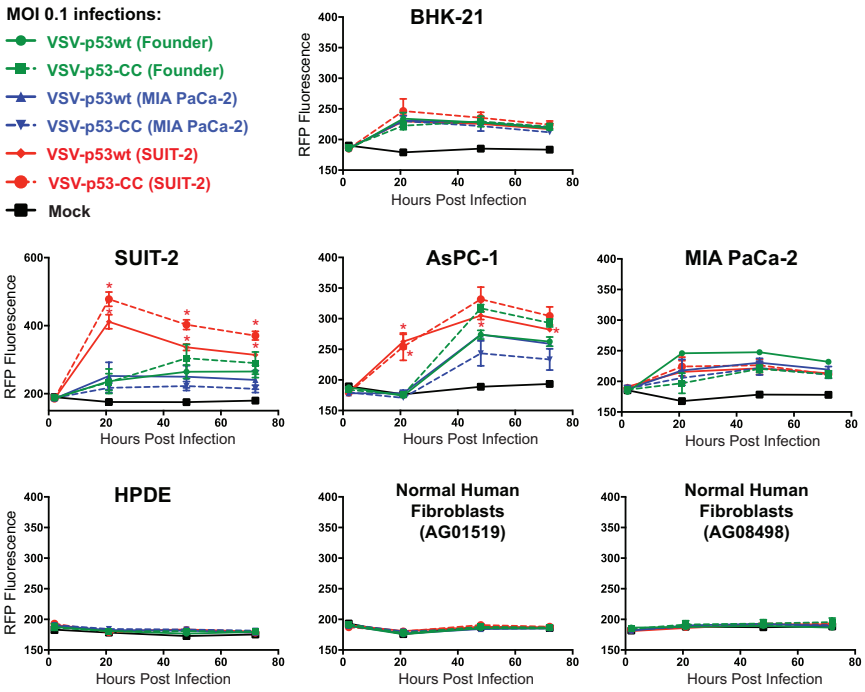

Figure 6. Viral replication kinetics of the founder and Passage 33 viruses.

Cell lines were either mock treated or infected with a virus at an MOI of 0.1 PFU/cell (MOI calculated based on virus titration on BHK-21). The level of VSV-encoded RFP fluorescence was measured over time from 1 h p.i. to 72 h p.i. The figure presents data representative of results from 2 independent experiments. Data points and error bars shown represent the means and SD of the means, respectively. *, $P < 0.05$; **, $P < 0.01$; ***, $P < 0.001$; ****, $P < 0.0001$; ns, nonsignificant. Results were analyzed to determine significance using two-way ANOVA with a Tukey posttest at a 95% confidence interval for comparison between each condition. If no error bars appear, the error is too small to appear on the graph.

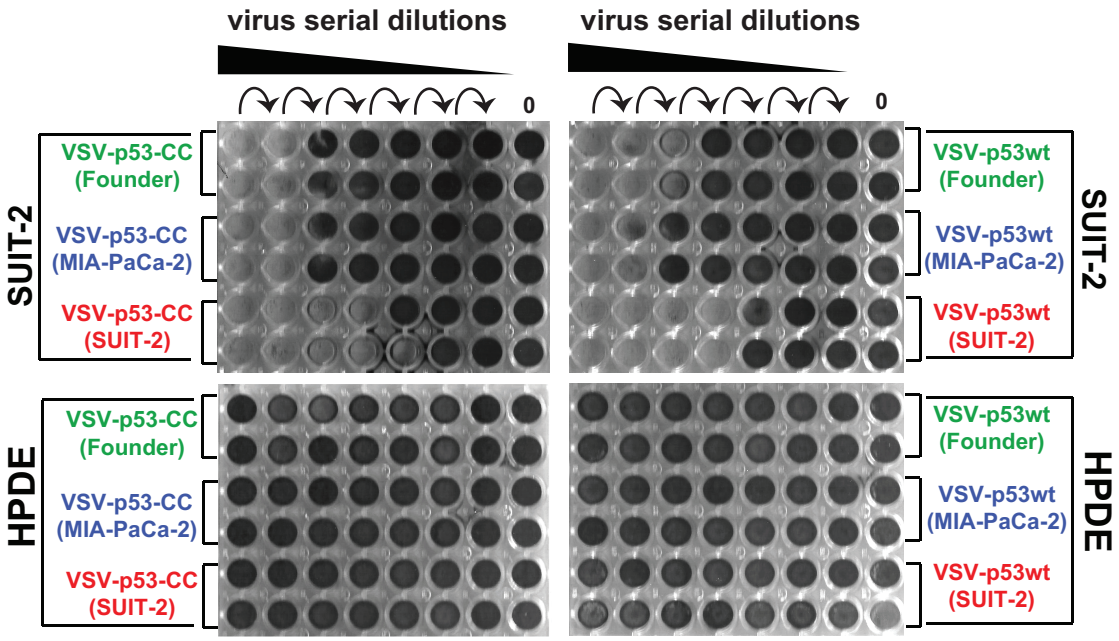

Figure 7. Crystal violet cytotoxicity assay.

The first well (on the left of each plate) was infected at MOI 0.15 (PFUs calculated based on virus titration on BHK-21), and then 6-fold serial dilutions were used to infect different cell lines in a 96-well format. Each cell line was also mock treated (control). Cells were stained with crystal violet solution (2% crystal violet in methanol) at 72 h p.i. to detect cytotoxicity caused by viruses, and unstained wells represent those in which total cell lysis had occurred. Figure shown is representative of results from at least two independent experiments.

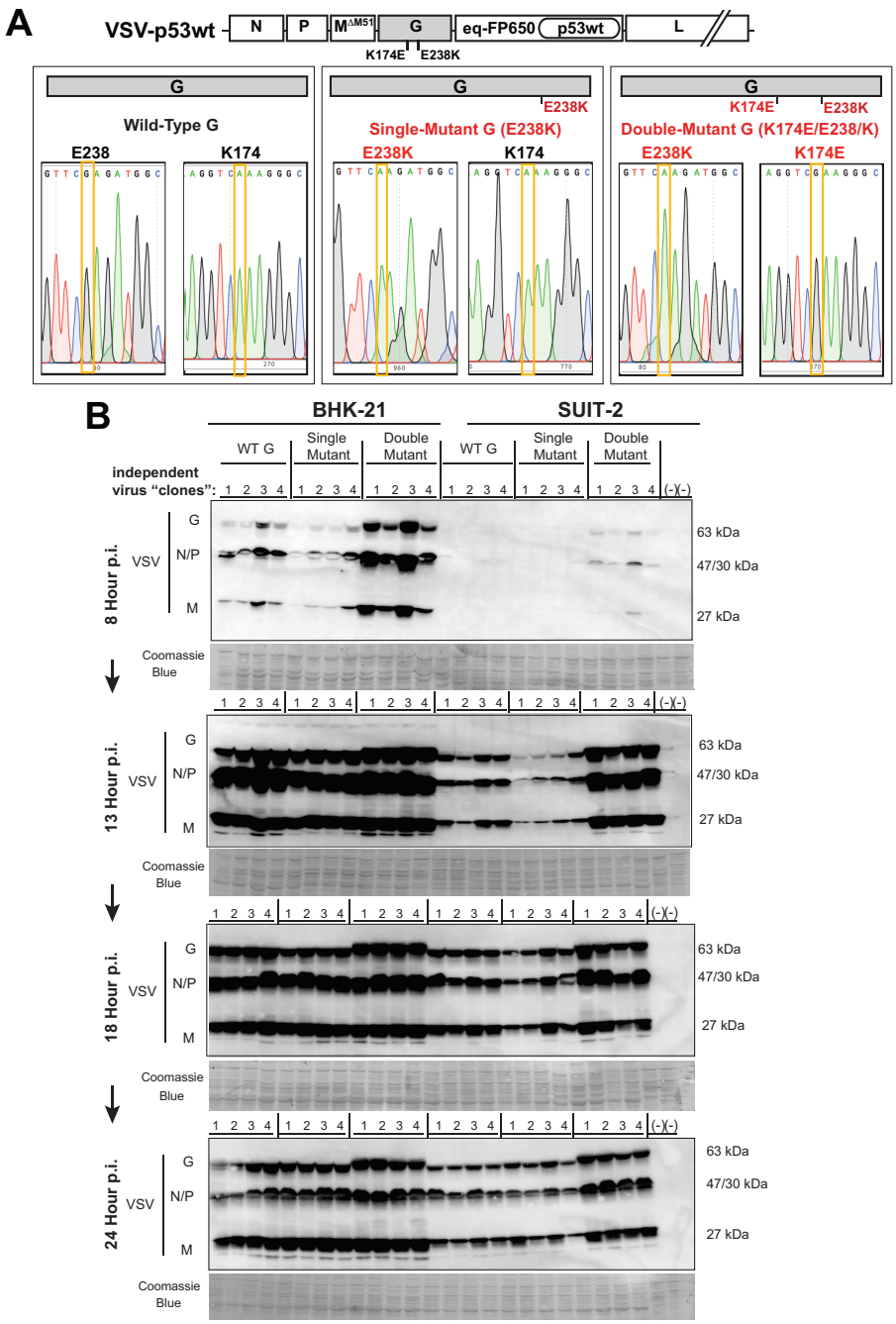

Figure 8. Generation and replication of single and double mutant plaque isolated viruses.

(A) Generation of VSV-p53wt viruses with WT G, Single Mutant (E238K) G and Double Mutant (K174E/E238K) G. Eight independent plaque-isolated VSV-p53wt viruses were obtained by serial dilution of Passage 20 (4 WT G and 4 Single Mutant E238K) as well as

4 passage 33 (Double Mutant K174E/E238K) plaque isolated viruses were generated from virus stocks until only 1 FFU was microscopically observed, then each virus originated from a single FFU was amplified in BHK-21 cells. Supernatants containing viral particles for the shown passages were used to isolate viral genomic RNA that was reversed transcribed into cDNA using random hexamers. This cDNA was PCR amplified using the primers VG383 and VG384 (described in Table 1) and the VSV-G regions containing aa positions 238 and 174 were sequenced. The nucleotide substitutions are highlighted in yellow boxes and the presence of either mutation is indicated by a red arrow above the sequences. (B) BHK-21 and SUIT-2 cell monolayers were incubated with each virus at an MOI of 0.1 (MOI calculated based on virus titration on BHK-21). Protein isolates were analyzed at 8, 13, 18, and 24 h p.i., and analyzed by western blotting for expression of VSV proteins (G, N/P, and M). Lane number indicated above membranes. Equal loading indicated by Coomassie Blue. Protein sizes are indicated on the side in kilodaltons (kDa).

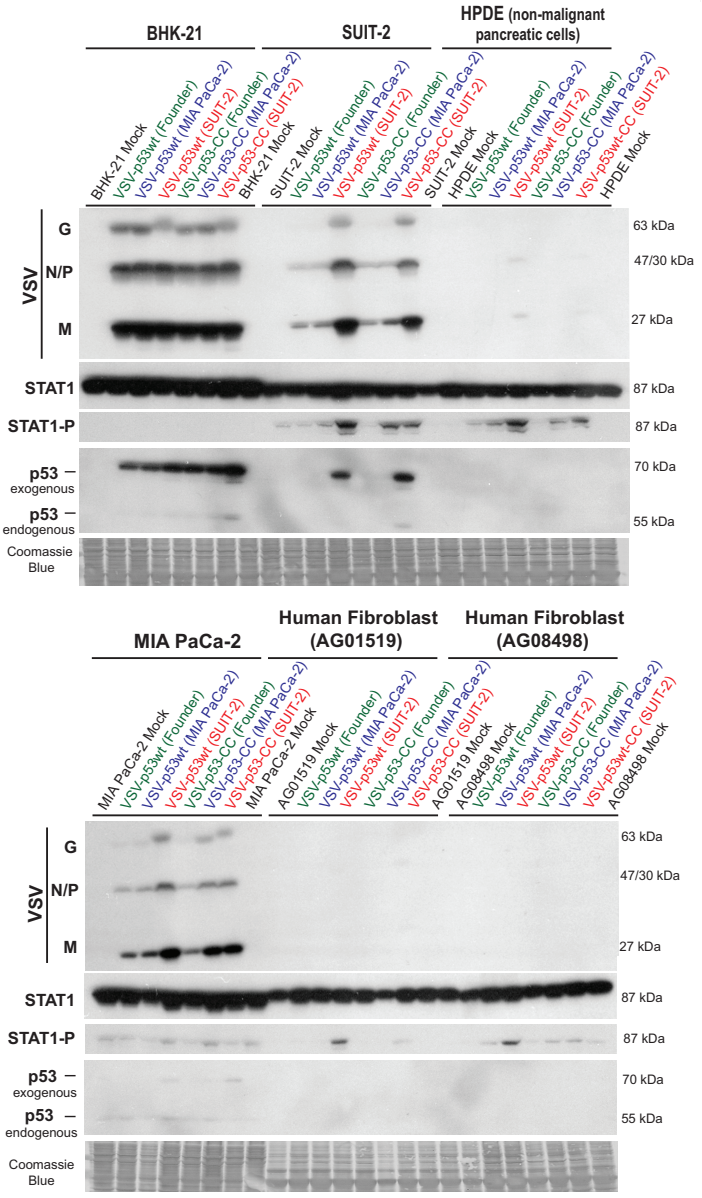

Figure 9. Replication of the founder and passage 33 viruses in different cell lines.

Cell monolayers of different cell lines were incubated with VSV-p53wt (Founder), VSV-p53-CC (Founder), VSV-p53wt (MIA PaCa-2), VSV-p53-CC (MIA PaCa-2), VSV-p53wt (SUIT-2) and, VSV-p53-CC (SUIT-2) at an MOI of 0.1 (MOI calculated based on virus

titration on BHK-21). Protein isolate was analyzed at 13 h p.i., were analyzed by western blotting for total STAT-1, phospho-STAT1 (STAT1-P), endogenous p53 (cell-encoded), exogenous p53 (virus-encoded RFP-p53 fusion), and VSV proteins (N, P, M and G). Equal loading indicated by Coomassie Blue. Protein sizes are indicated on the side in kilodaltons (kDa).

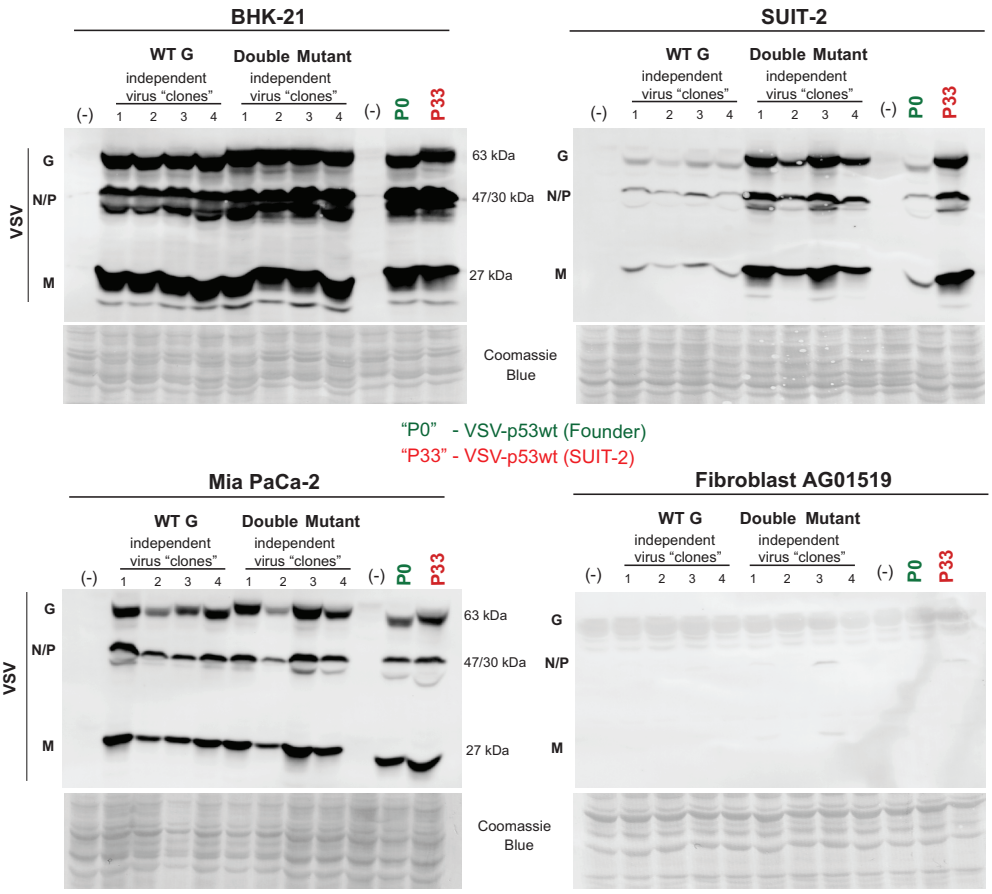

Figure 10. Replication of single and double mutant plaque isolated viruses in different cell lines to examine oncoselectivity.

Comparing replication of VSV-p53wt (Founder), VSV-p53wt (SUIT-2) and plaque isolated VSV with WT VSV-G, Single Mutant (E238K) VSV-G and Double Mutant

(K174E/E238K) VSV-G. Cell monolayers of different cell lines were incubated with either the original founder virus (P0) or passage 33 virus (P33) or the plaque isolated viruses at an MOI of 0.1 (MOI calculated based on virus titration on BHK-21). Protein isolates were analyzed at 13 h p.i., and analyzed by western blotting for VSV proteins (N, P, M and G). Equal loading indicated by Coomassie Blue. Protein sizes are indicated on the side in kilodaltons (kDa).

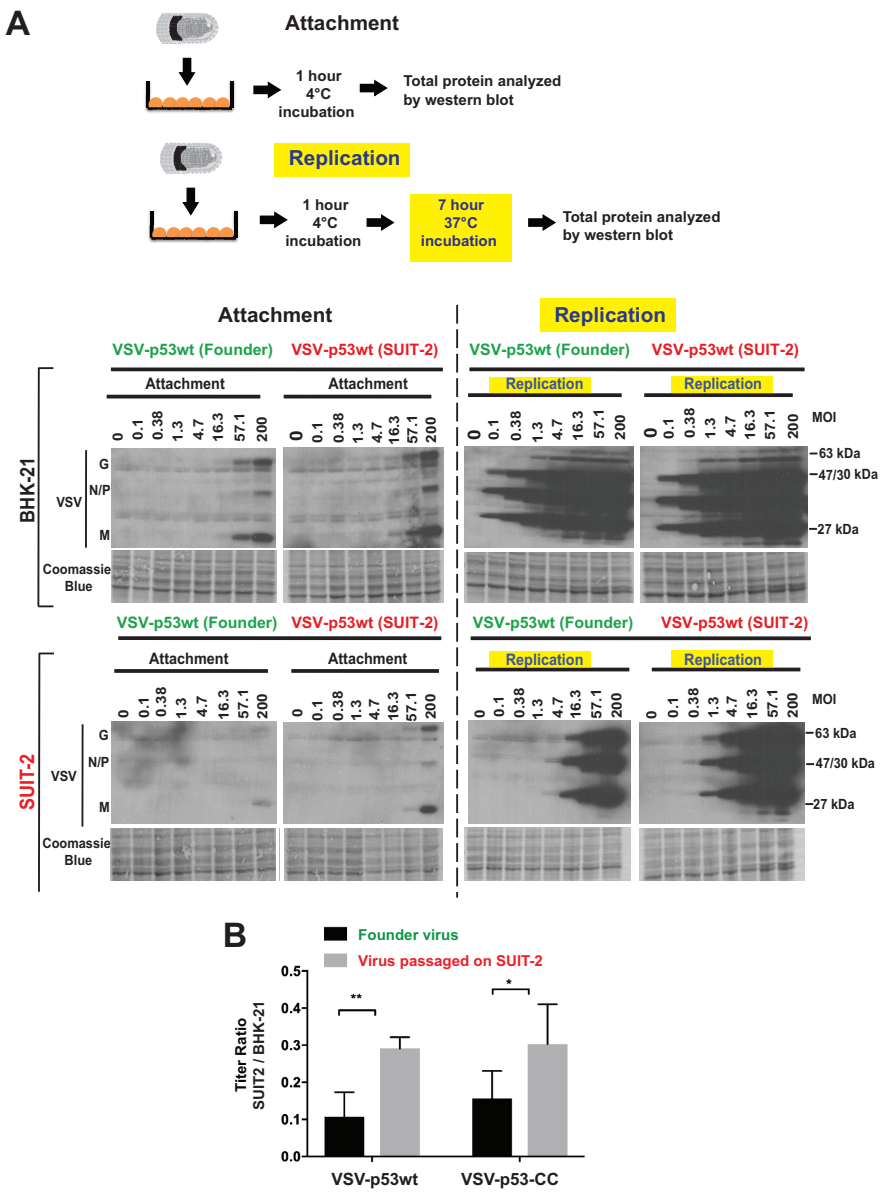

Figure 11. Comparing VSV attachment and replication in BHK-21 and SUIT-2 cells.

(A) For VSV attachment to cells in monolayers, cells were incubated with purified VSV-p53wt (Founder) or VSV-p53wt (SUIT-2). Cell monolayers were incubated with either virus at different MOI (calculated based on virus titration on BHK-21) for 1 h at 4°C (Attachment assay) only or for 1 h at 4°C and then additional 7 h at 37°C (Replication

assay). Protein was isolated and analyzed by western blotting. Coomassie Blue stain was used to indicate equal loading of samples. Protein sizes are indicated on the side in kilodaltons (kDa). (B) Virus titers on both SUIT-2 and BHK-21 cells compared for VSV-p53wt (Founder) compared to VSV-p53wt (SUIT-2) as well as VSV-p53-CC (Founder) compared to VSV-p53-CC (SUIT-2). Data bars and error bars represent the means and SD of the means, respectively. Data represent the means and SD of the means. Conditions were compared using unpaired t-tests of at least 3 repeated experiments. *, $P < 0.05$; **, $P < 0.01$; ***, $P < 0.001$; ****, $P < 0.0001$; ns, nonsignificant.

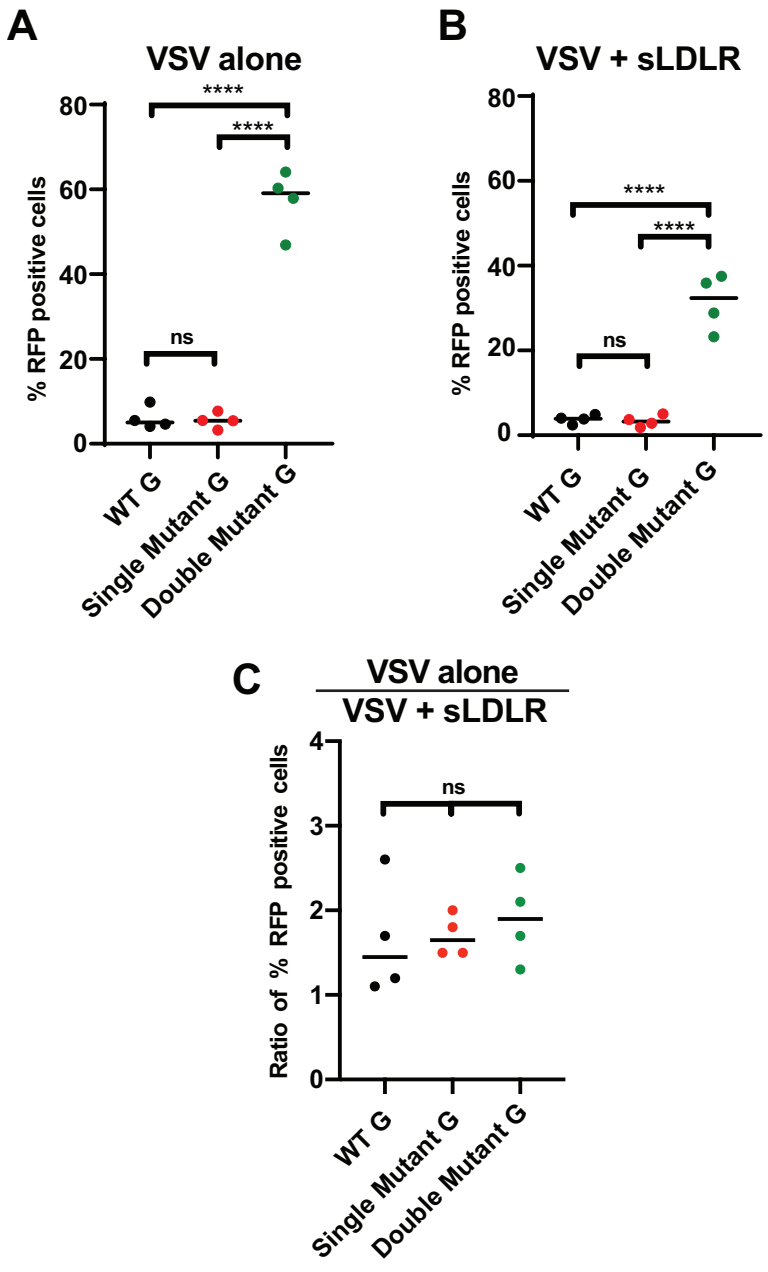

Figure 12. Effect of sLDLR on infectivity of VSV-p53wt viruses with WT G, Single Mutant (E238K) G and Double Mutant (K174E/E238K) G.

Four independent plaque-isolated VSV-p53wt viruses were obtained by serially diluting passage 20 (WT G and Single Mutant E238K) or passage 33 (Double Mutant K174E/E238K) virus stocks until only 1 FFU was microscopically observed, then each

virus originated from a single FFU was amplified in BHK-21 cells. MOI 0.1 virus dilutions were incubated without sLDLR (A) or with 1 μg/mL sLDLR (B) for 30 min at 37°C before being used in SUIT-2 infection (calculated based on virus titration on BHK-21). After a 30 min infection, virus containing media was removed and fresh media was added. 13 h p.i. RFP positive cells were counted using a Nexcelom Vision Image Cytometer. The data presented is representative of two independent experiments. Data points and error bars shown represent the means and SD of the means, respectively. Results were analyzed to determine significance using one-way ANOVA with a Tukey posttest at a 95% confidence interval for comparison between each condition. *, $P < 0.05$; **, $P < 0.01$; ***, $P < 0.001$; ****, $P < 0.0001$; ns, nonsignificant. (C) Percent of RFP infected cells in the presence of sLDLR divided by percent of RFP infected cells without sLDLR compared to determine the relative inhibition sLDLR has on WT, Single Mutant and Double Mutant VSVs.

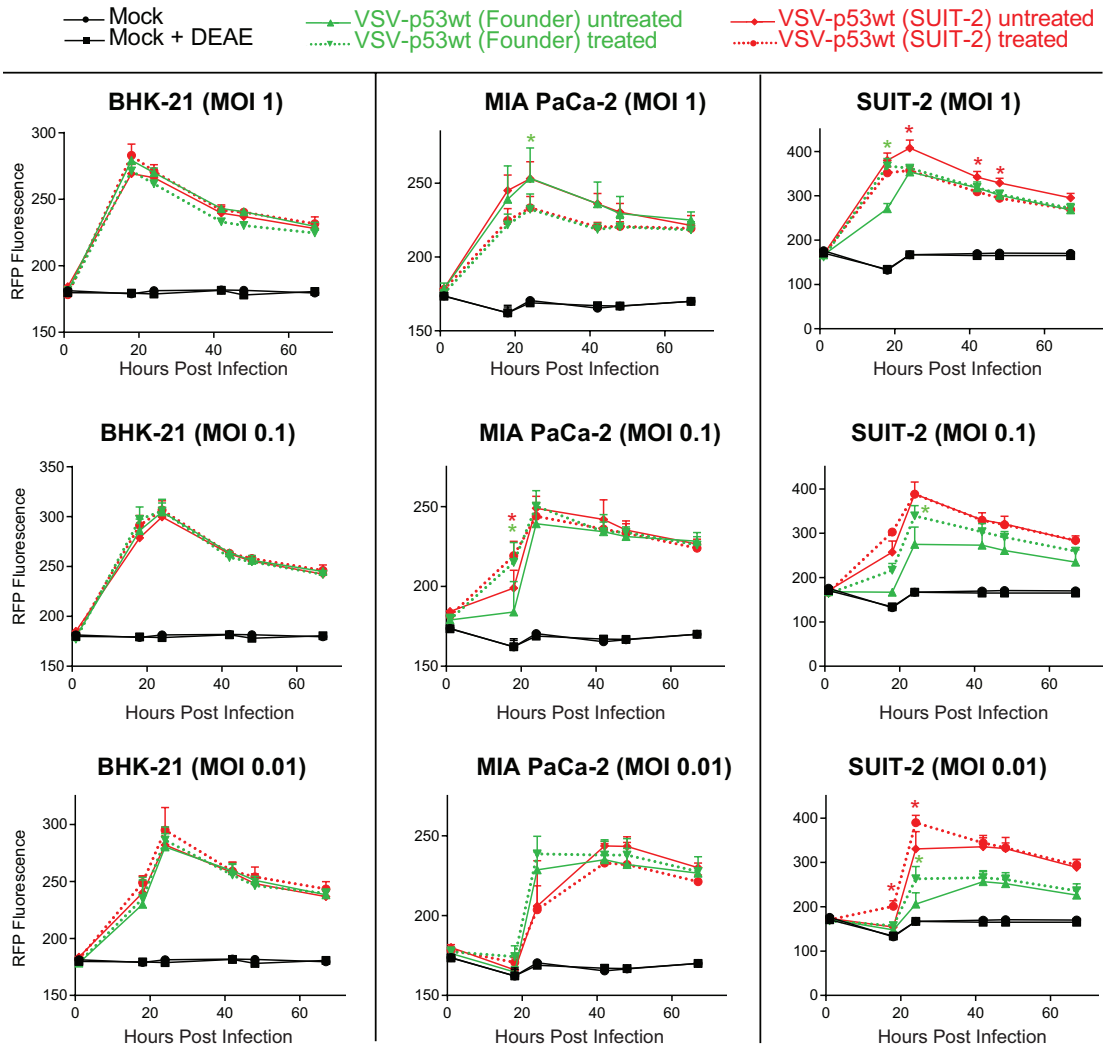

Figure 13. Effect of polycation DEAE-dextran on VSV infection in different cell lines.

Cells were pretreated with 10 µg/ml DEAE-dextran or mock treated for 30 min, and then infected with indicated virus at an MOI of either 1, 0.1 or 0.01 (MOI calculated based on virus titration on BHK-21) for 1 h at 37°C. Virus + DEAE-dextran containing media were removed after the 1 h infection period and fresh DMEM with 5% FBS was added to the cells. The level of VSV-encoded RFP fluorescence was measured over the course of 68. The figure presents data representative of results from 3 independent experiments. Data points and error bars shown represent the means and SD of the means, respectively. Results

were analyzed to determine significance using two-way ANOVA with a Tukey posttest at a 95% confidence interval for comparison between each condition. *, $P < 0.05$; **, $P < 0.01$; ***, $P < 0.001$; ****, $P < 0.0001$; ns, nonsignificant. If no error bars appear, the error is too small to appear on the graph.

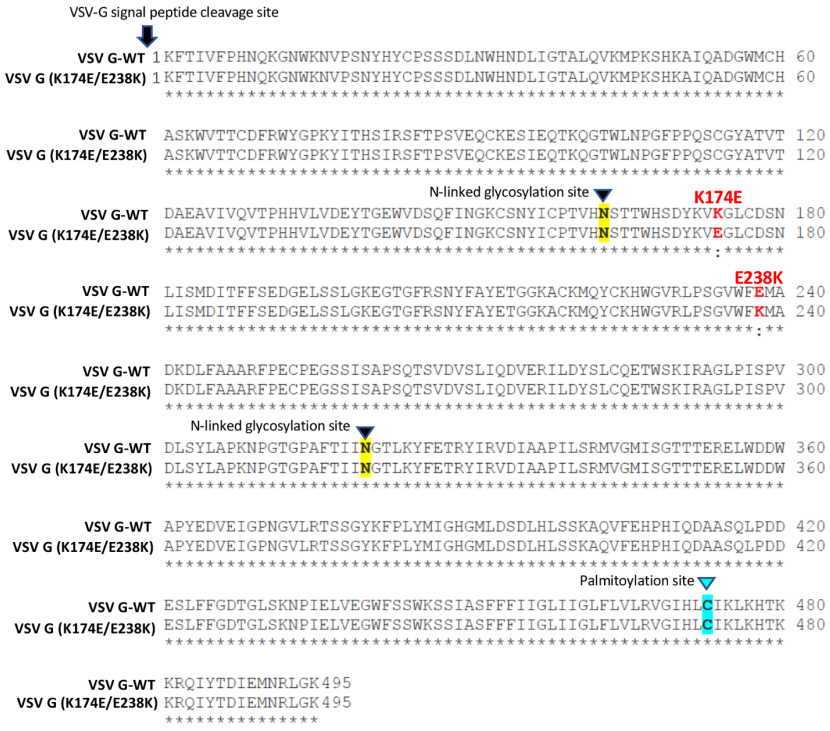

Figure 14. Sequence comparison of WT VSV-G and mutant VSV-G.

Sequence comparison of VSV WT VSV-G (NCBI GenBank Sequence ID: FJ478454.1) and Double Mutant VSV-G. The aa numbering is starting from the first aa of the mature VSV-G and does not include 16-aa N-terminal signal peptide. The positions of the identified mutations, as well as known VSV-G N-glycosylation and palmitoylation are indicated.

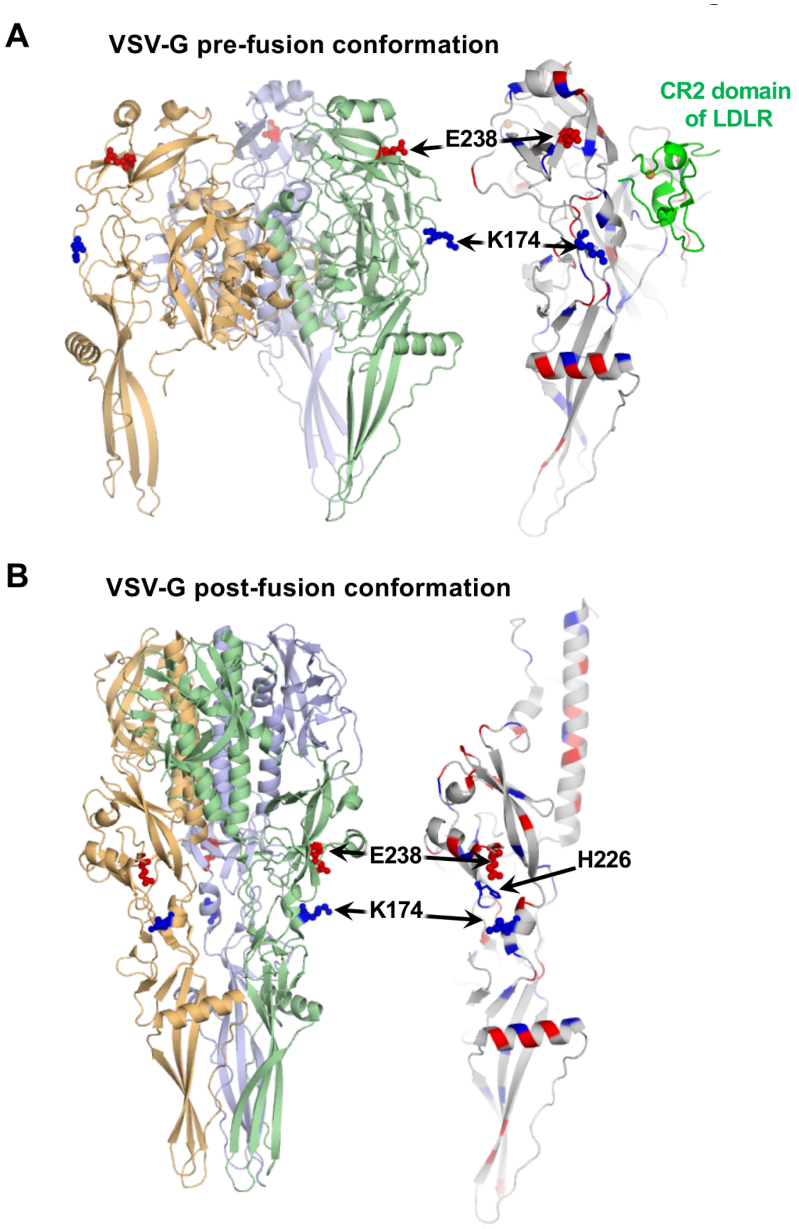

Figure 15. Location of VSV-G E238K and K174E mutations on crystallographic structures of pre-fusion and post-fusion states of the glycoprotein G.

(A) Representation of the prefusion conformation of protein G bound to the cysteine-rich domain of LDL receptor. Positively and negatively charged residues are shown by blue and red color, respectively. E238 and K174 are shown using sticks and spheres. E238 is surrounded by positively charged residues. Both E238 and K174 are positioned away from

the binding interface of VSV-G and LDLR CR2 region. (B) Representation of low-pH, post-fusion conformation of VSV-G trimer (left) and VSV-G monomer (right). Color-coding is the same as in panel A. Both E238 and K174 are positioned away from the intermonomer interface in the protein VSV-G trimer (left). Histidine H226 is sandwiched by E238 and K174 (right).

3.4 Discussion

These experimental evolution experiments employed two different oncolytic VSV recombinants, VSV-p53wt and VSV-p53-CC, previously generated in our laboratory (Hastie et al., 2015) (Fig. 2A). Both viruses have a ΔM51 mutation in VSV-M, and the N terminus of p53 (p53wt or p53-CC) fused to the C terminus of RFP (Shcherbo et al., 2007). One important advantage of using p53 transgenes in this study is that this protein functions normally as a powerful tumor suppressor (and this is why p53 is often added to other therapies, including OV therapy, to augment their antitumor activity), however, when mutated, p53 can acquire devastating gain-of-function oncogenic activities, promoting cell survival, proliferation, invasion, migration, chemoresistance, tissue remodeling and chronic inflammation (Bressy et al., 2017). Therefore, our experimental design also allowed us to monitor if VSV-encoded p53 transgenes could acquire such mutations during extensive passaging on cancer cells. Passaging two different VSV recombinants that have the same ΔM51 attenuation and RFP transgene but different p53 variants allowed us to ensure there was no viral cross-contamination over the course of the parallel viral passaging, as the differences between p53wt and p53-CC served as “molecular barcodes” for each recombinant virus while still offering a type of biological repeat since the viruses have been shown to function very similarly (Hastie et al., 2015).

We serially passaged 2 founder viruses VSV-p53wt (Founder) and VSV-p53-CC (Founder), which were produced by BHK-21 cells (a highly permissive baby hamster kidney cell line widely used for VSV amplification), in parallel on two different human PDAC cell lines, SUIT-2 and MIA PaCa-2 (Fig. 2A). The cell lines SUIT-2 and MIA PaCa-2 were chosen because of their differential permissiveness to VSV and other differences (Fig. 2B). SUIT-2 cells are more resistant to VSV infection in part because of residual type I IFN responses, yet permissive enough to support sufficient viral replication to produce enough viral progeny for continued viral passaging, while MIA PaCa-2 cells are very permissive to VSV infection in part due to their inactive type I IFN signaling (Bressy et al., 2019; Hastie et al., 2015; Moerdyk-Schauwecker et al., 2013). Also, we showed that SUIT-2 cells showed lower levels of VSV attachment, compared to MIA PaCa-2 (Felt et al., 2017). Each virus has a large transgene (about 17% of WT VSV genome) encoding a different version of p53 fused to RFP. Regarding p53, a previous study from our lab showed that VSV-encoding p53 could stimulate VSV replication in cancer cells with active type I IFN signaling, such as SUIT-2 cells, but had no effect on VSV replication in MIA PaCa-2 cells that are defective in type I IFN signaling (Hastie et al., 2015). This was at least in part because p53 was able to inhibit type I IFN signaling in SUIT-2 cells thus facilitating viral replication (Hastie et al., 2015). The RFP reporter sequences are presumably dispensable for VSV replication in both cell lines, and previous studies suggest that the addition of a reporter transgene to VSV genome slightly attenuates viral replication (Wertz et al., 2002). However, nucleotide (nt) substitutions or deletions in the RFP coding region could negatively affect p53 expression or function as the N terminus of p53 (p53wt or p53-CC) fused to the C terminus of RFP in both viruses (Shcherbo et al., 2007). In

general, while we expected stronger selective pressures in SUIT-2 cells, both viruses could improve viral replication by losing at least some transgenic sequences due to random mutations as it would reduce the time it takes to replicate the viral genome and assemble virions.

Over the course of 33 viral passages all viruses retained both the p53 (p53wt or p53-CC) and RFP sequences of the virus-encoded transgenes. No transgenes in any of the viruses obtained any mutations demonstrating long-term genomic stability of complex VSV recombinants encoding large transgenes even after replicating over an extended period of time (more than 768 h of continuous viral replication). The result is surprising considering that neither p53 nor RFP expression would presumably benefit VSV-ΔM51 replication in MIA PaCa-2 cells, although p53 expression stimulates VSV-ΔM51 replication in SUIT-2 cells via inhibition of antiviral signaling (Hastie et al., 2015).

RNA viruses are known to have high mutation rates due to a lack of proofreading activities by viral RNA-dependent RNA polymerase (Lauring et al., 2013; Steinhauer et al., 1992). This lack of proofreading can result in the introduction of mutations in the form of nucleotide changes or frameshift mutations in the viral genome or transgenic regions. Such mutations can have a detrimental effect on the expression of viral or recombinant proteins. For instance, in a study where VSV expressed recombinant CD4 protein, a single deletion resulting in a frameshift mutation caused the loss of expression of the transgene that was seemingly stable after 26 passages (Quinones-Kochs et al., 2001/9/1). Another VSV recombinant from the same study carrying measles virus F protein lost the transgene after 1 passage. Several different factors may have contributed to the surprising transgenic stability of our tested viruses. First, while NNS RNA viruses, as any RNA viruses, are

associated with a high mutation rate (Lauring et al., 2013; Steinhauer et al., 1992), they show lower incidence of genetic recombination caused by polymerase slippage compared to positive-strand RNA viruses, because the viral genome in NNS RNA viruses is encapsidated at all times, as opposed to naked RNA genomes of positive-strand RNA viruses where polymerase can disassociate with one strand of RNA and re-associate on another strand (Collins et al., 2008; Pfaller et al., 2015). Second, the helical nucleocapsid and overall bullet shape of VSV can accommodate extra transgenes by adding length to the virus rather than being geometrically limited in icosahedral virions of some other viruses (Schnell et al., 1996a). Third, our transgene sequences were not fused to viral proteins, which could increase selective pressures to lose the transgene. Previously, an in-frame fusion of eGFP to VSV-P, an essential viral protein, resulted in the loss of transgene expression within 20 passages assumedly because the reporter gene resulted in reduced viral fitness (Dinh et al., 2012). Fourth, our viruses had transgene sequences located between VSV G and L genes. Although placing a transgene closer to the 3'-end of viral genome can increase its expression, it also results in greater virus attenuation (Pfaller et al., 2015; Roberts et al., 2004; van den Pol and Davis, 2013; Wertz et al., 2002), which increases the selective pressures to lose the transgene sequences. On the other hand, several studies have successfully inserted transgenes between the G and L proteins of both VSV and RABV without diminishing viral replication or activity (Hudacek et al., 2014; Mebatsion et al., 1996; Schnell et al., 1996b; Wertz et al., 2002). Finally, the observed stability of the RFP-p53 transgenes is likely due to the selective pressures associated with beneficial effect of p53 expression on VSV replication in PDAC cells. As mentioned above, our previous study showed that these VSV-encoded p53 transgenes enhanced VSV

anti-cancer abilities through the introduction of functional p53 into cancer cells with defective tumor suppression activity and through the downregulation of antiviral signaling in cancer cells, while stimulating it in normal cells (Hastie et al., 2015). Although this positive effect was observed only in SUIT-2 cells, but not in MIA PaCa-2 cells that have an overall defective antiviral signaling (Hastie et al., 2015), the fact that p53 transgene was stable in both cell lines after 33 passages suggest that p53 has at least a minor positive effect on VSV replication even in MIA PaCa-2 cells or that MIA PaCa-2 offer no significant selective pressure to remove or mutate these transgenes resulting in their retention at least for 33 passages.

Both of the SUIT-2 passaged viruses acquired more mutations than the Mia PaCa-2 passaged viruses, likely because of the stronger selective pressures in SUIT-2 (compared to Mia PaCa-2) cells. Most of the mutations found in the SUIT-2 passaged viruses were in VSV-G, a trend that has been observed in other VSV evolution studies (Alto et al., 2013). Interestingly 2 identical missense mutations were identified in both VSV-p53wt (SUIT-2) and VSV-p53-CC (SUIT-2) in the VSV-G gene at positions E238K and K174E. We confirmed these mutations were in fact independently generated in each lineage by sequencing the p53 region of multiple different passages of the viruses which showed no contamination of the p53 regions. VSV-p53-CC (SUIT-2) also showed a third missense mutation in VSV-G, M184I, but only in a portion of the passage 33 VSV-p53-CC population. Although it will be interesting to examine the role of this mutation in VSV replication in the future studies, it is unlikely that this particular mutation plays a critical role in the improved ability of this virus to replicate in SUIT-2 cells, as VSV-p53wt (SUIT-2) and VSV-p53-CC (SUIT-2) exhibited very similar

phenotypes. Therefore, our studies focused on E238K and K174E mutations. Only the viruses passaged on VSV-resistant SUIT-2 cells obtained the mutations E238K and K174E in VSV-G, indicating SUIT-2 but not MIA PaCa-2 cells provided the selective pressure required for complete fixation of these two mutations within VSV populations. This could indicate that more permissive cell lines may not be conducive for a directed evolution approach to further improve OV therapy.

Interestingly, both viruses first obtained the E238K mutation around passage 10, well before acquiring the K174E mutation (around passage 26). We observed rapid fixation of E238K after detection of K174E in viral populations, and both VSV-p53wt (SUIT-2) and VSV-p53-CC (SUIT-2) completely switched to the mutant genotype by passage 32. When several independent plaque-purified "clones" of VSV-p53wt with no G mutations, a single E238K mutation and both K174E and E238K mutations were isolated and compared, we observed that the improved replication phenotype required the presence of the E238K and K174E mutation. It is likely that the first mutations, E238K, provided a minor fitness benefit to both, VSV-p53wt and VSV-p53-CC, founder viruses, but the observed major shift in virus replication required both mutations. It should be noted that the second mutation, K174E, was never identified alone in any of the viral passages and thus was not individually. While it is beyond the scope of this study, it will be interesting to generate and examine such virus in the future studies.

Although the double VSV-G mutant E238K/K174E has never been described in the past, a previous study described VSV-G mutants E238G (VSV mutants "G_6" and "G_{6R}") and E238Q (VSV mutants "G_5" and "G_{5R}") (Janelle et al., 2011). Most of these previously described VSV mutants had additional mutations in VSV-G, although one of the mutants,

VSV G_{6R}, had only the single aa substitution E238G in VSV-G (Janelle et al., 2011). The study showed that VSV G_{6R} infection of L929 cells (mouse fibroblasts) produced higher levels of IFN-β, compared to WT VSV, and those levels were similar to or even higher than that with the VSV-M51R mutant. Based on that result, the authors proposed that E238G mutation in VSV-G enhances type I interferon secretion and responses via some unclear mechanism not involving VSV-M (Janelle et al., 2011). However, we propose another explanation for their observations, that E238G mutation may have resulted in an improved replication of VSV G_{6R} virus in L929 cells, and the observed overall increase in IFN-β was due to the increase in the number of infected cells rather than the increased IFN-β production by each infected cell. In agreement with this hypothesis, the previous study did not detect any attenuation of VSV G_{6R} replication in L929 cells expected for a mutant, which replication enhances antiviral response (Janelle et al., 2011). Our data also show the increased antiviral response for viruses with the acquired G mutations, but perhaps that stronger IFN response was due to higher levels of VSV replication which we observed throughout this study. In general, we observed a proportional increase in STAT1 phosphorylation as viral replication increased in cell lines with active antiviral signaling indicating that VSV-p53wt (SUIT-2) and VSV-p53-CC (SUIT-2) are not modulating antiviral signaling in each cell, but the higher number of infected cells produce collectively a stronger antiviral response.

Although we cannot exclude additional mechanisms of the improved VSV replication in the presence of E238K and K174E mutations in VSV-G, our data show that these mutations result in an improved VSV attachment to SUIT-2 cells. Interestingly, our previous study showed that SUIT-2 cells show lower levels of attachment for VSV,

compared to MIA PaCa-2 (Felt et al., 2017). Therefore, we presume that during VSV passaging, when a virus passage was incubated with fresh cells for 1 h period (after which the incubation media containing unbound virus was aspirated and cells washed with PBS), there was a selective pressure for VSV mutants capable for more efficient attachment to SUIT-2 cells.

It is unclear how the E238K and K174E mutations in VSV-G improve VSV attachment to PDAC cells. We analyzed the position of E238K and K174E mutations using the crystallographic structures of prefusion conformations of VSV-G with and without LDLR (pdb codes 5oyl, 5oy9, 5i2s) and low-pH, post-fusion conformations of VSV-G without LDLR (pdb code 2cmz) (Nikolic et al., 2018; Roche et al., 2006; Roche et al., 2007) (Fig. 14 and 15). As shown in Figure 15, both mutations are located away from the interaction interface between VSV-G and the CR2 or CR3 (cysteine-rich) domains of LDLR. Both mutations are also located on the side of the protein opposite to the intermonomer interface in the post-fusion trimer. Therefore, it is unlikely that they affect the trimerization of the glycoprotein G or its interaction with LDLR, at least with the CR2 or CR3 domains for which x-ray structures have been solved. In agreement with that, we did not detect any significant differences between WT and mutant G viruses in regard to the inhibiting effect of sLDLR on viral infectivity (Fig. 12C). Also, our previous study showed that, despite lower levels of VSV attachment to SUIT-2 cells, SUIT-2 expressed high levels of LDLR, suggesting no limitation of the surface receptor for VSV in this cell line (Felt et al., 2017). Together, these data suggest that VSV-G mutations did not dramatically alter the abilities of mutant VSV-G proteins to attach to and infect SUIT-2 cells through an interaction with LDLR.

Interestingly, our data indicate that the VSV G mutations E238K and K174E make the evolved viruses less dependent on polycations for efficient infection of SUIT-2. Previous studies have suggested that efficient cell attachment of virions of many viruses, including VSV and VSV-G-pseudotyped viruses (Akkina et al., 1996; Burns et al., 1993), requires an initial non-specific binding of virus particles to cell surface, followed by attachment of virus particles to their specific receptors, which is required for virus internalization (Denning et al., 2013; Pizzato et al., 1999; Reiser et al., 1996; Sharma et al., 2000; Yee et al., 1994). The initial non-specific binding step can be dramatically enhanced by treating cells with polycations, such as DEAE-dextran or polybrene (Bailey et al., 1984; Conti et al., 1991; Matlin et al., 1982). Importantly, we have previously shown that infectivity of VSV-ΔM51 in several resistant PDAC cell lines, including SUIT-2, was dramatically improved when cells were treated with the polycations DEAE-dextran or polybrene (Felt et al., 2017). Although the exact mechanism of polycation-mediated improvement of virion attachment is not clear and several alternative mechanisms, including charge shielding and virus aggregation, have been proposed (Davis et al., 2004), the most widely-accepted hypothesis is that polycations decrease electrostatic repulsion between negatively charged molecules on the surface of cells and many viruses, including VSV, and thus facilitate nonspecific binding of virus particles to cell surface (Bailey et al., 1984; Conti et al., 1991; Davis et al., 2002). Our data indicate that the VSV G mutations E238K and K174E make the evolved viruses less dependent on polycations possibly by decreasing dissociation of virions at the initial step of attachment due to electrostatic repulsion between cell surface molecules and VSV. One possibility is that these mutations change the overall structure of VSV-G that would significantly change charge distribution

on the surface of VSV particles. Alternatively, these mutations could change post-translational modifications (PTMs) of VSV-G. Both glutamic acid (E238) and especially lysine (K174) could be potentially modified by PTM, and, in addition, K174E or E238K mutations could alter the PTMs of other VSV-G aa residues. At least two types of PTMs have been identified in VSV-G: N-glycosylation through N163 and N320 positions and palmitoylation through a cysteine residue C473 in the cytoplasmic tail domain (Rose et al., 1984; Scheiffele et al., 1999; Whitt and Rose, 1991) (Fig. 13). Although the biological role of VGV-G palmitoylation is still unclear, VSV GP (G) contains two well conserved N-glycosylation sites, N163 and N320 (Fig. 13), which make up to approximately 10% of the VSV-G mass (Etchison and Holland, 1974; Farley et al., 2007; Ortega et al., 2019; Puri et al., 1992; Reading et al., 1978; Robertson et al., 1978; Rose and Gallione, 1981; Stanley et al., 1984). The VGV-G N-glycosylation can dramatically affect viral infectivity, although the effect strongly depends on target cell type and specific mode of VSV-G N-glycosylation (Farley et al., 2007; Marozin et al., 2012; Ortega et al., 2019). It is believed that one of the major mechanisms of DEAE-dextran-mediated improvement of VSV infection is removal of repulsion between negatively-charged molecules on the cell surface (such as anionic phospholipids sialic acid residues) and terminal sialic acid residues associated with those N-glycosylated VSV-G (Ortega et al., 2019). It is possible that E238K and K174E or mutations could alter VSV-G N-glycosylation pattern or juxtaposition of sialic acid residues and thus decrease repulsion, thus making mutant viruses less dependent on DEAE-dextran for virus infection.

We cannot rule out that E238K and K174E VSV-G mutations also affect other steps of virus replication cycle. VSV-G is responsible for both viral attachment and entry into

host cells and it is possible one or both of these mutations not only improved attachment, but also virus entry into the infected cells. Interestingly, E238K and K174E mutations are located near the region that undergoes the major conformational rearrangement during the transition from pre-fusion to post-fusion state. It is possible that these mutations play a role in this transition. E238 and K174 are about 24 Å apart in the prefusion conformation, but only about 10 Å apart in the post-fusion conformation. As mentioned before, in all passages, we found that the E238K mutation occurred prior to K174E mutation. E238 is located on the central beta-strand of the DIII (pleckstrin homology, PH) domain and is surrounded by positively charged residues including K44, K220, K225, H226, and K242 (Figure 14). The substitution of E238 for lysine would disturb the balance of positive and negative charge in this region, which could potentially lead to a conformational rearrangement. Furthermore, in a post-fusion conformation, a histidine residue H226 is positioned between E238 and K174 residues, with the distance of 4 Å and 7 Å between the sidechains of H226 and of E238 and K174, respectively. Therefore, it is plausible to assume that the K174 mutation is a “rescue” mutation that re-establishes the balance of positive and negative charge around the histidine, which could be important for the conformational transition from prefusion to post-fusion state. Future studies will test these possibilities.

CHAPTER 4: CONCLUSION

After serially passaging 2 VSV recombinants, VSV-p53wt and VSV-p53-CC to investigate if VSV can be directionally evolved to better kill PDAC cell lines, clear phenotypic differences were identified as the viruses passaged on SUIT-2 cells 33 times exhibited an improved ability to replicate in and kill SUIT-2 cells. Evidence for this includes viral kinetics where VSV-p53wt (SUIT-2) and VSV-p53-CC (SUIT-2) were able to replicate more quickly and to a higher level in SUIT-2 cells than the original founder viruses as well as through western blot analysis comparing viral protein accumulation over the course of multiple time points with the same trend identified. End point dilutions were also utilized to determine cell cytotoxicity of the founder and passage 33 viruses which also indicate that the viruses passaged on SUIT-2 cells have an improved ability to kill SUIT-2 cells compared to the founder viruses or the viruses passaged 33 times on MIA PaCa-2 cells. Taken together, this is evidence that both VSV-p53wt and VSV-p53-CC can be directionally evolved to replicate in and kill semi-resistant cancer cell lines such as SUIT-2. VSV-p53wt (SUIT-2) and VSV-p53-CC (SUIT-2) exhibited similar phenotypes on the PDAC cell lines AsPC-1, another semi-resistant PDAC with similar characteristics to SUIT-2, such as residual type I IFN signaling. This further indicates VSVs ability to be adapted to resistant PDAC cell lines to improve their therapeutical abilities for the treatment of cancer.

This work supports further research and development of OVs carrying transgenes as all passaged viruses showed complete retention of both a p53wt or p53-CC transgene after extensive viral passaging in 2 different malignant cell lines. While it is not known how other selective pressures such as a patients adaptive immune response or the

complexities of a tumor microenvironment might alter transgene stability of OVs, this work supports future studies which might examine these other factors. In the future, it would be interesting to examine the efficacy of VSV-p53wt (SUIT-2) and VSV-p53-CC (SUIT-2) *in vivo*. This is currently limited by a lack of an appropriate PDAC mouse model as human PDAC cell lines cannot be used in an immunocompetent mouse. *In vivo* studies are further complicated because the p53 transgenes incorporated into our viruses are human derived which have different responses than murine p53 (Horvath et al., 2007).

Both identical missense mutations being independently acquired by VSV-p53wt (SUIT-2) and VSV-p53-CC (SUIT-2) in VSV-G, E238K and K174E suggests a strong benefit to VSV in SUIT-2 cells from the introduction of these mutations. To further characterize the role these mutations play in improving VSV replication in SUIT-2 and AsPC-1 cell lines, it would be interesting for future studies to examined each mutation in both WT VSV and VSV-ΔM51. This would allow for the mutations to be evaluated separately from any potential influence from the presence of the p53 transgenes.

Due to our experimental design where each viral passage was incubated for a 1 h incubation period, previous data that indicates VSV attaches less to SUIT-2 cells than other PDAC cell lines, and our current data on VSV-p53wt (SUIT-2) and VSV-p53-CC (SUIT-2) improved ability to attach to SUIT-2 cells, we suggest that the E238K and K174E mutations have altered VSV-G so as to interact with SUIT-2 cells more efficiently at the level of virus attachment to host cell. While other mechanisms such as virus fusion could be involved, our current hypothesis is furthered by the lack of improvement from

polycation treatment which indicates that these mutations result in VSV-G improve VSVs ability to interact with SUIT-2 cell surface.

In conclusion, from the work presented in this thesis, VSV can be directionally evolved to specify and target OV treatment to a target PDAC cell line while also widening the scope of an OV to a specific cancer type to more than one cell line. This has implications for the improvement and development of more personalized cancer treatment options especially for chemoresistant and overall difficult to treat cancers such as PDAC. This work also provides evidence that the use of transgenes in OV therapy appear to be stably expressed and retained within a viral genome without the accumulatio of mutations over undergoing at least 66 viral replication cycles.

REFERENCES

Adamska, A., Domenichini, A., Falasca, M., 2017. Pancreatic Ductal Adenocarcinoma: Current and Evolving Therapies. Int J Mol Sci 18.

Ahmed, M., McKenzie, M.O., Puckett, S., Hojnacki, M., Poliquin, L., Lyles, D.S., 2003. Ability of the matrix protein of vesicular stomatitis virus to suppress beta interferon gene expression is genetically correlated with the inhibition of host RNA and protein synthesis. J Virol 77, 4646-4657.

Akkina, R.K., Walton, R.M., Chen, M.L., Li, Q.X., Planelles, V., Chen, I.S., 1996. High-efficiency gene transfer into CD34+ cells with a human immunodeficiency virus type 1-based retroviral vector pseudotyped with vesicular stomatitis virus envelope glycoprotein G. J Virol 70, 2581-2585.

Alto, B.W., Wasik, B.R., Morales, N.M., Turner, P.E., 2013. Stochastic temperatures impede RNA virus adaptation. Evolution 67, 969-979.

Amirache, F., Levy, C., Costa, C., Mangeot, P.E., Torbett, B.E., Wang, C.X., Negre, D., Cosset, F.L., Verhoeyen, E., 2014. Mystery solved: VSV-G-LVs do not allow efficient gene transfer into unstimulated T cells, B cells, and HSCs because they lack the LDL receptor. Blood 123, 1422-1424.

Ammayappan, A., Peng, K.W., Russell, S.J., 2013. Characteristics of oncolytic vesicular stomatitis virus displaying tumor-targeting ligands. J Virol 87, 13543-13555.

Ayala-Breton, C., Suksanpaisan, L., Mader, E.K., Russell, S.J., Peng, K.W., 2013. Amalgamating oncolytic viruses to enhance their safety, consolidate their killing mechanisms, and accelerate their spread. Mol Ther 21, 1930-1937.

Bailey, C.A., Miller, D.K., Lenard, J., 1984. Effects of DEAE-dextran on infection and hemolysis by VSV. Evidence that nonspecific electrostatic interactions mediate effective binding of VSV to cells. Virology 133, 111-118.

Bailey, M.J., McLeod, D.A., Kang, C.Y., Bishop, D.H., 1989. Glycosylation is not required for the fusion activity of the G protein of vesicular stomatitis virus in insect cells. Virology 169, 323-331.

Balachandran, S., Barber, G.N., 2004. Defective translational control facilitates vesicular stomatitis virus oncolysis. Cancer Cell 5, 51-65.

Baltimore, D., 1971. Expression of animal virus genomes. Bacteriol Rev 35, 235-241.
Barber, G.N., 2004. Vesicular stomatitis virus as an oncolytic vector. Viral Immunol 17, 516-527.

Bauzon, M., Hermiston, T.W., 2012. Oncolytic viruses: the power of directed evolution. Adv Virol 2012, 586389.

Bi, Z., Quandt, P., Komatsu, T., Barna, M., Reiss, C.S., 1995. IL-12 promotes enhanced recovery from vesicular stomatitis virus infection of the central nervous system. J immunol 155, 5684-5689.

Black, B.L., Lyles, D.S., 1992. Vesicular stomatitis virus matrix protein inhibits host cell-directed transcription of target genes in vivo. J Virol 66, 4058-4064.

Black, B.L., Rhodes, R.B., McKenzie, M., Lyles, D.S., 1993. The role of vesicular stomatitis virus matrix protein in inhibition of host-directed gene expression is genetically separable from its function in virus assembly. J Virol 67, 4814-4821.

Boritz, E., Gerlach, J., Johnson, J.E., Rose, J.K., 1999. Replication-competent rhabdoviruses with human immunodeficiency virus type 1 coats and green fluorescent protein: entry by a pH-independent pathway. J Virol 73, 6937-6945.

Bressy, C., Droby, G.N., Maldonado, B.D., Steuerwald, N., Grdzelishvili, V.Z., 2019. Cell Cycle Arrest in G2/M Phase Enhances Replication of Interferon-Sensitive Cytoplasmic RNA Viruses via Inhibition of Antiviral Gene Expression. J Virol 93.

Bressy, C., Hastie, E., Grdzelishvili, V.Z., 2017. Combining Oncolytic Virotherapy with p53 Tumor Suppressor Gene Therapy. Molecular Therapy-Oncolytics 5, 20-40.

Brown, C.W., Stephenson, K.B., Hanson, S., Kucharczyk, M., Duncan, R., Bell, J.C., Lichty, B.D., 2009. The p14 FAST protein of reptilian reovirus increases vesicular stomatitis virus neuropathogenesis. J Virol 83, 552-561.

Bukreyev, A., Skiadopoulos, M.H., Murphy, B.R., Collins, P.L., 2006. Nonsegmented negative-strand viruses as vaccine vectors. J Virol 80, 10293-10306.

Burns, J.C., Friedmann, T., Driever, W., Burrascano, M., Yee, J.K., 1993. Vesicular stomatitis virus G glycoprotein pseudotyped retroviral vectors: concentration to very high titer and efficient gene transfer into mammalian and nonmammalian cells. Proc Natl Acad Sci U S A 90, 8033-8037.

Carneiro, F.A., Lapido-Loureiro, P.A., Cordo, S.M., Stauffer, F., Weissmuller, G., Bianconi, M.L., Juliano, M.A., Juliano, L., Bisch, P.M., Da Poian, A.T., 2006. Probing the interaction between vesicular stomatitis virus and phosphatidylserine. Eur Biophys J 35, 145-154.

Cataldi, M., Shah, N.R., Felt, S.A., Grdzelishvili, V.Z., 2015. Breaking resistance of pancreatic cancer cells to an attenuated vesicular stomatitis virus through a novel activity of IKK inhibitor TPCA-1. Virology 485, 340-354.

Clarke DK, N.F., Lee M, Johnson JE, Wright K, Calderon P, Guo M, Natuk R, Cooper D, Hendry RM, Udem SA., 2007. Synergistic attenuation of vesicular stomatitis virus by combination of specific G gene truncations and N gene translocations. Journal of Virology 81, 2056-2064.

Coil, D.A., Miller, A.D., 2004. Phosphatidylserine is not the cell surface receptor for vesicular stomatitis virus. J Virol 78, 10920-10926.

Collins, P.L., Bukreyev, A., Murphy, B.R., 2008. What are the risks--hypothetical and observed--of recombination involving live vaccines and vaccine vectors based on nonsegmented negative-strain RNA viruses? J Virol 82, 9805-9806.

Conti, C., Mastromarino, P., Riccioli, A., Orsi, N., 1991. Electrostatic interactions in the early events of VSV infection. Res Virol 142, 17-24.

Coulon, P., Deutsch, V., Lafay, F., Martinet-Edelist, C., Wyers, F., Herman, R.C., Flamand, A., 1990. Genetic evidence for multiple functions of the matrix protein of vesicular stomatitis virus. J Gen Virol 71 (Pt 4), 991-996.

Davis, H.E., Morgan, J.R., Yarmush, M.L., 2002. Polybrene increases retrovirus gene transfer efficiency by enhancing receptor-independent virus adsorption on target cell membranes. Biophys Chem 97, 159-172.

Davis, H.E., Rosinski, M., Morgan, J.R., Yarmush, M.L., 2004. Charged polymers modulate retrovirus transduction via membrane charge neutralization and virus aggregation. Biophys J 86, 1234-1242.

Davis, J.N., van den Pol, A.N., 2010. Viral mutagenesis as a means for generating novel proteins. J Virol 84, 1625-1630.
Denning, W., Das, S., Guo, S., Xu, J., Kappes, J.C., Hel, Z., 2013. Optimization of the transductional efficiency of lentiviral vectors: effect of sera and polycations. Mol Biotechnol 53, 308-314.

Dinh, P.X., Panda, D., Das, P.B., Das, S.C., Das, A., Pattnaik, A.K., 2012. A single amino acid change resulting in loss of fluorescence of eGFP in a viral fusion protein confers fitness and growth advantage to the recombinant vesicular stomatitis virus. Virology 432, 460-469.

Draper, S.J., Heeney, J.L., 2010. Viruses as vaccine vectors for infectious diseases and cancer. Nat Rev Microbiol 8, 62-73.

Ebert O, Harbaran S, Shinozaki K, and Woo, S.L., 2005. Systemic therapy of experimental breast cancer metastases by mutant vesicular stomatitis virus in immune-competent mice. Cancer Gene Therapy 12, 350-358.

Etchison, J.R., Holland, J.J., 1974. Carbohydrate composition of the membrane glycoprotein of vesicular stomatitis virus grown in four mammalian cell lines. Proc Natl Acad Sci U S A 71, 4011-4014.

Farley, D.C., Iqball, S., Smith, J.C., Miskin, J.E., Kingsman, S.M., Mitrophanous, K.A., 2007. Factors that influence VSV-G pseudotyping and transduction efficiency of lentiviral vectors-in vitro and in vivo implications. J Gene Med 9, 345-356.

Felt, S.A., Droby, G.N., Grdzelishvili, V.Z., 2017. Ruxolitinib and Polycation Combination Treatment Overcomes Multiple Mechanisms of Resistance of Pancreatic Cancer Cells to Oncolytic Vesicular Stomatitis Virus. J Virol 91.

Felt, S.A., Grdzelishvili, V.Z., 2017. Recent advances in vesicular stomatitis virus-based oncolytic virotherapy: a 5-year update. Journal of General Virology 98, 2895-2911.
Felt, S.A., Moerdyk-Schauwecker, M.J., Grdzelishvili, V.Z., 2015. Induction of apoptosis in pancreatic cancer cells by vesicular stomatitis virus. Virology 474, 163-173.

Finke, S., Conzelmann, K.K., 2005. Recombinant rhabdoviruses: vectors for vaccine development and gene therapy. Curr Top Microbiol Immunol 292, 165-200.

Finkelshtein, D., Werman, A., Novick, D., Barak, S., Rubinstein, M., 2013. LDL receptor and its family members serve as the cellular receptors for vesicular stomatitis virus. Proc Natl Acad Sci USA 110, 7306-7311.

Freedman, J.D., Duffy, M.R., Lei-Rossmann, J., Muntzer, A., Scott, E.M., Hagel, J., Campo, L., Bryant, R.J., Verrill, C., Lambert, A., Miller, P., Champion, B.R., Seymour, L.W., Fisher, K.D., 2018. An Oncolytic Virus Expressing a T-cell Engager Simultaneously Targets Cancer and Immunosuppressive Stromal Cells. Cancer Res 78, 6852-6865.

Furukawa T, Duguid WP, Rosenberg L, Viallet J, Galloway DA, and Tsao, M.S., 1996. Long-term culture and immortalization of epithelial cells from normal adult human pancreatic ducts transfected by the E6E7 gene of human papilloma virus 16. The American Journal of Pathology 148, 1763-1770.

Gao, Y., Whitaker-Dowling, P., Watkins, S.C., Griffin, J.A., Bergman, I., 2006. Rapid adaptation of a recombinant vesicular stomatitis virus to a targeted cell line. J Virol 80, 8603-8612.

Garijo, R., Hernandez-Alonso, P., Rivas, C., Diallo, J.S., Sanjuan, R., 2014. Experimental evolution of an oncolytic vesicular stomatitis virus with increased selectivity for p53-deficient cells. PLoS One 9, e102365.

Giri, B., Sethi, V., Dudeja, V., Banerjee, S., Livingstone, A., Saluja, A., 2017. Genetics of pancreatic cyst-cancer progression: standing on the shoulders of giants. Curr Opin Gastroenterol 33, 404-410.

Guibinga, G.H., Miyanohara, A., Esko, J.D., Friedmann, T., 2002. Cell surface heparan sulfate is a receptor for attachment of envelope protein-free retrovirus-like particles and VSV-G pseudotyped MLV-derived retrovirus vectors to target cells. Mol Ther 5, 538-546.
Habjan, M., Penski, N., Spiegel, M., Weber, F., 2008. T7 RNA polymerase-dependent and -independent systems for cDNA-based rescue of Rift Valley fever virus. J Gen Virol 89, 2157-2166.

Hastie, E., Cataldi, M., Marriott, I., Grdzelishvili, V.Z., 2013. Understanding and altering cell tropism of vesicular stomatitis virus. Virus research 176, 16-32.

Hastie, E., Cataldi, M., Moerdyk-Schauwecker, M.J., Felt, S.A., Steuerwald, N., Grdzelishvili, V.Z., 2016. Novel biomarkers of resistance of pancreatic cancer cells to oncolytic vesicular stomatitis virus. Oncotarget 7, 61601-61618.

Hastie, E., Cataldi, M., Steuerwald, N., Grdzelishvili, V.Z., 2015. An unexpected inhibition of antiviral signaling by virus-encoded tumor suppressor p53 in pancreatic cancer cells. Virology 483, 126-140.

Hastie, E., Grdzelishvili, V.Z., 2012. Vesicular stomatitis virus as a flexible platform for oncolytic virotherapy against cancer. J Gen Virol 93, 2529-2545.

Heiber, J.F., Barber, G.N., 2011. Vesicular stomatitis virus expressing tumor suppressor p53 is a highly attenuated, potent oncolytic agent. J Virol 85, 10440-10450.

Hernandez-Alonso, P., Garijo, R., Cuevas, J.M., Sanjuan, R., 2015. Experimental evolution of an RNA virus in cells with innate immunity defects. Virus Evol 1, vev008.

Horvath, M.M., Wang, X., Resnick, M.A., Bell, D.A., 2007. Divergent evolution of human p53 binding sites: cell cycle versus apoptosis. PLoS genetics 3, e127.

Hudacek, A.W., Al-Saleem, F.H., Willet, M., Eisemann, T., Mattis, J.A., Simpson, L.L., Schnell, M.J., 2014. Recombinant rabies virus particles presenting botulinum neurotoxin antigens elicit a protective humoral response in vivo. Mol Ther Methods Clin Dev 1, 14046.
Iwamura T, Katsuki T, K., I., 1987. Establishment and characterization of a human pancreatic cancer cell line (SUIT-2) producing carcinoembryonic antigen and carbohydrate antigen 19-9. Jpn J Cancer Res. 78, 54-62.

Janelle, V., Brassard, F., Lapierre, P., Lamarre, A., Poliquin, L., 2011. Mutations in the glycoprotein of vesicular stomatitis virus affect cytopathogenicity: potential for oncolytic virotherapy. J Virol 85, 6513-6520.

Johnson JE, Nasar F, Coleman JW, Price RE, Javadian A, Draper K, Lee M, Reilly PA, Clarke DK, Hendry RM, Udem, S.A., 2007. Neurovirulence properties of recombinant vesicular stomatitis virus vectors in non-human primates. Virology 360, 36-49.

Kandoth, C., McLellan, M.D., Vandin, F., Ye, K., Niu, B., Lu, C., Xie, M., Zhang, Q., McMichael, J.F., Wyczalkowski, M.A., Leiserson, M.D., Miller, C.A., Welch, J.S., Walter, M.J., Wendl, M.C., Ley, T.J., Wilson, R.K., Raphael, B.J., Ding, L., 2013. Mutational landscape and significance across 12 major cancer types. Nature 502, 333-339.

Ke, Y., Yu, D., Zhang, F., Gao, J., Wang, X., Fang, X., Wang, H., Sun, T., 2019. Recombinant vesicular stomatitis virus expressing the spike protein of genotype 2b porcine epidemic diarrhea virus: A platform for vaccine development against emerging epidemic isolates. Virology 533, 77-85.

Kelly, E., Russell, S.J., 2007. History of oncolytic viruses: genesis to genetic engineering. Molecular therapy : the journal of the American Society of Gene Therapy 15, 651-659.
Koonin, E.V., 2010. The wonder world of microbial viruses. Expert Rev Anti Infect Ther 8, 1097-1099.

Kuhn, I., Bauzon, M., Green, N., Seymour, L., Fisher, K., Hermiston, T., 2017. OvAd1, a Novel, Potent, and Selective Chimeric Oncolytic Virus Developed for Ovarian Cancer by 3D-Directed Evolution. Mol Ther Oncolytics 4, 55-66.

Kuhn, I., Harden, P., Bauzon, M., Chartier, C., Nye, J., Thorne, S., Reid, T., Ni, S., Lieber, A., Fisher, K., Seymour, L., Rubanyi, G.M., Harkins, R.N., Hermiston, T.W., 2008. Directed evolution generates a novel oncolytic virus for the treatment of colon cancer. PLoS One 3, e2409.

Lauring, A.S., Frydman, J., Andino, R., 2013. The role of mutational robustness in RNA virus evolution. Nat Rev Microbiol 11, 327-336.

Letchworth, G.J., Rodriguez, L.L., Del cbarrera, J., 1999. Vesicular stomatitis. The Veterinary Journal 157, 239-260.

Lichty BD, Power AT, Stojdl DF, and Bell, J.C., 2004. Vesicular stomatitis virus: re-inventing the bullet. Trends Mol Med 10, 210-216.

Lin, D.M., Koskella, B., Lin, H.C., 2017. Phage therapy: An alternative to antibiotics in the age of multi-drug resistance. World J Gastrointest Pharmacol Ther 8, 162-173.

Lyles DS, R., CE, 2007. Rhabdoviridae, in: In: DM Knipe and PM Howley, e. (Ed.), Fields Virology. Lippincott Williams & Wilkins, Philadelphia, 5th edition., pp. 1363-1408.

Machamer, C.E., Florkiewicz, R.Z., Rose, J.K., 1985. A single N-linked oligosaccharide at either of the two normal sites is sufficient for transport of vesicular stomatitis virus G protein to the cell surface. Molecular & Cellular Biology 5, 3074-3083.

Marozin, S., Altomonte, J., Apfel, S., Dinh, P.X., De Toni, E.N., Rizzani, A., Nussler, A., Kato, N., Schmid, R.M., Pattnaik, A.K., Ebert, O., 2012. Posttranslational modification of

vesicular stomatitis virus glycoprotein, but not JNK inhibition, is the antiviral mechanism of SP600125. J Virol 86, 4844-4855.

Marozin, S., Altomonte, J., Stadler, F., Thasler, W.E., Schmid, R.M., Ebert, O., 2008. Inhibition of the IFN-beta response in hepatocellular carcinoma by alternative spliced isoform of IFN regulatory factor-3. Mol Ther 16, 1789-1797.

Marozin, S., De Toni, E.N., Rizzani, A., Altomonte, J., Junger, A., Schneider, G., Thasler, W.E., Kato, N., Schmid, R.M., Ebert, O., 2010. Cell cycle progression or translation control is not essential for vesicular stomatitis virus oncolysis of hepatocellular carcinoma. PLoS One 5, e10988.

Martinez, I., Wertz, G.W., 2005. Biological differences between vesicular stomatitis virus Indiana and New Jersey serotype glycoproteins: identification of amino acid residues modulating pH-dependent infectivity. J Virol 79, 3578-3585.

Matlin, K.S., Reggio, H., Helenius, A., Simons, K., 1982. Pathway of vesicular stomatitis virus entry leading to infection. J Mol Biol 156, 609-631.

Mebatsion, T., Schnell, M.J., Cox, J.H., Finke, S., Conzelmann, K.K., 1996. Highly stable expression of a foreign gene from rabies virus vectors. Proc Natl Acad Sci U S A 93, 7310-7314.

Moerdyk-Schauwecker, M., Shah, N.R., Murphy, A.M., Hastie, E., Mukherjee, P., Grdzelishvili, V.Z., 2013. Resistance of pancreatic cancer cells to oncolytic vesicular stomatitis virus: role of type I interferon signaling. Virology 436, 221-234.

Moussavi, M., Fazli, L., Tearle, H., Guo, Y., Cox, M., Bell, J., Ong, C., Jia, W., Rennie, P.S., 2010. Oncolysis of prostate cancers induced by vesicular stomatitis virus in PTEN knockout mice. Cancer Res 70, 1367-1376.

Murphy, A.M., Besmer, D.M., Moerdyk-Schauwecker, M., Moestl, N., Ornelles, D.A., Mukherjee, P., Grdzelishvili, V.Z., 2012. Vesicular stomatitis virus as an oncolytic agent against pancreatic ductal adenocarcinoma. J Virol 86, 3073-3087.

Nikolic, J., Belot, L., Raux, H., Legrand, P., Gaudin, Y., A, A.A., 2018. Structural basis for the recognition of LDL-receptor family members by VSV glycoprotein. Nat Commun 9, 1029.

Novella, I.S., 2003. Contributions of vesicular stomatitis virus to the understanding of RNA virus evolution. Curr Opin Microbiol 6, 399-405.

Okal, A., Mossalam, M., Matissek, K.J., Dixon, A.S., Moos, P.J., Lim, C.S., 2013. A chimeric p53 evades mutant p53 transdominant inhibition in cancer cells. Mol Pharm 10, 3922-3933.

Ortega, V., Stone, J.A., Contreras, E.M., Iorio, R.M., Aguilar, H.C., 2019. Addicted to sugar: roles of glycans in the order Mononegavirales. Glycobiology 29, 2-21.
Otsuki, K., Maeda, J., Yamamoto, H., Tsubokura, M., 1979. Studies on avian infectious bronchitis virus (IBV). III. Interferon induction by and sensitivity to interferon of IBV. Arch Virol 60, 249-255.

Paul, S., Ricour, C., Sommereyns, C., Sorgeloos, F., Michiels, T., 2007. Type I interferon response in the central nervous system. Biochimie 89, 770-778.
Perlmutter, J.D., Hagan, M.F., 2015. Mechanisms of virus assembly. Annu Rev Phys Chem 66, 217-239.

Pfaller, C.K., Cattaneo, R., Schnell, M.J., 2015. Reverse genetics of Mononegavirales: How they work, new vaccines, and new cancer therapeutics. Virology 479-480, 331-344.
Pizzato, M., Marlow, S.A., Blair, E.D., Takeuchi, Y., 1999. Initial binding of murine leukemia virus particles to cells does not require specific Env-receptor interaction. J Virol 73, 8599-8611.

Puri, A., Grimaldi, S., Blumenthal, R., 1992. Role of viral envelope sialic acid in membrane fusion mediated by the vesicular stomatitis virus envelope glycoprotein. Biochemistry 31, 10108-10113.

Quinones-Kochs, M.I., Schnell, M.J., Buonocore, L., Rose, J.K., 2001/9/1. Mechanisms of loss of foreign gene expression in recombinant vesicular stomatitis viruses. Virology 287, 427-435.

Reading, C.L., Penhoet, E.E., Ballou, C.E., 1978. Carbohydrate structure of vesicular stomatitis virus glycoprotein. The Journal of biological chemistry 253, 5600-5612.
Reiser, J., Harmison, G., Kluepfel-Stahl, S., Brady, R.O., Karlsson, S., Schubert, M., 1996. Transduction of nondividing cells using pseudotyped defective high-titer HIV type 1 particles. Proc Natl Acad Sci U S A 93, 15266-15271.

Reiss, C.S., Plakhov, I.V., Komatsu, T., 1998. Viral replication in olfactory receptor neurons and entry into the olfactory bulb and brain. Ann NY Acad Sci 855, 751-761.
Rice, A., Del Rio Hernandez, A., 2019. The Mutational Landscape of Pancreatic and Liver Cancers, as Represented by Circulating Tumor DNA. Front Oncol 9, 952.

Roberts, A., Reuter, J.D., Wilson, J.H., Baldwin, S., Rose, J.K., 2004. Complete protection from papillomavirus challenge after a single vaccination with a vesicular stomatitis virus vector expressing high levels of L1 protein. J Virol 78, 3196-3199.

Robertson, J.S., Etchison, J.R., Summers, D.F., 1976. Glycosylation sites of vesicular stomatitis virus glycoprotein. J Virol 19, 871-878.

Robertson, M.A., Etchison, J.R., Robertson, J.S., Summers, D.F., Stanley, P., 1978. Specific changes in the oligosaccharide moieties of VSV grown in different lectin-resistnat CHO cells. Cell 13, 515-526.

Roche, S., Bressanelli, S., Rey, F.A., Gaudin, Y., 2006. Crystal structure of the low-pH form of the vesicular stomatitis virus glycoprotein G. Science 313, 187-191.

Roche, S., Rey, F.A., Gaudin, Y., Bressanelli, S., 2007. Structure of the prefusion form of the vesicular stomatitis virus glycoprotein G. Science 315, 843-848.

Rose, J.K., Adams, G.A., Gallione, C.J., 1984. The presence of cysteine in the cytoplasmic domain of the vesicular stomatitis virus glycoprotein is required for palmitate addition. Proc Natl Acad Sci U S A 81, 2050-2054.

Rose, J.K., Gallione, C.J., 1981. Nucleotide sequences of the mRNA's encoding the vesicular stomatitis virus G and M proteins determined from cDNA clones containing the complete coding regions. J Virol 39, 519-528.

Russell, S.J., Peng, K.W., Bell, J.C., 2012. Oncolytic virotherapy. Nat Biotechnol 30, 658-670.

Sanjuan, R., Grdzelishvili, V.Z., 2015. Evolution of oncolytic viruses. Curr Opin Virol 13c, 1-5.

Scheiffele, P., Rietveld, A., Wilk, T., Simons, K., 1999. Influenza viruses select ordered lipid domains during budding from the plasma membrane. J Biol Chem 274, 2038-2044.
Schlegel, R., Tralka, T.S., Willingham, M.C., Pastan, I., 1983. Inhibition of VSV binding and infectivity by phosphatidylserine: is phosphatidylserine a VSV-binding site? Cell 32, 639-646.

Schloemer, R.H., Wagner, R.R., 1975. Cellular adsorption function of the sialoglycoprotein of vesicular stomatitis virus and its neuraminic acid. J Virol 15, 882-893.
Schnell, M.J., Buonocore, L., Kretzschmar, E., Johnson, E., Rose, J.K., 1996a. Foreign glycoproteins expressed from recombinant vesicular stomatitis viruses are incorporated efficiently into virus particles. Proc Natl Acad Sci U S A 93, 11359-11365.

Schnell, M.J., Buonocore, L., Whitt, M.A., Rose, J.K., 1996b. The minimal conserved transcription stop-start signal promotes stable expression of a foreign gene in vesicular stomatitis virus. J Virol 70, 2318-2323.

Sharma, S., Miyanohara, A., Friedmann, T., 2000. Separable mechanisms of attachment and cell uptake during retrovirus infection. J Virol 74, 10790-10795.

Shcherbo, D., Merzlyak, E.M., Chepurnykh, T.V., Fradkov, A.F., Ermakova, G.V., Solovieva, E.A., Lukyanov, K.A., Bogdanova, E.A., Zaraisky, A.G., Lukyanov, S., Chudakov, D.M., 2007. Bright far-red fluorescent protein for whole-body imaging. Nature methods 4, 741-746.

Simovic, B., Walsh, S.R., Wan, Y., 2015. Mechanistic insights into the oncolytic activity of vesicular stomatitis virus in cancer immunotherapy. Oncolytic Virother 4, 157-167.

Sinn, B.V., Striefler, J.K., Rudl, M.A., Lehmann, A., Bahra, M., Denkert, C., Sinn, M., Stieler, J., Klauschen, F., Budczies, J., Weichert, W., Stenzinger, A., Kamphues, C., Dietel, M., Riess, H., 2014. KRAS mutations in codon 12 or 13 are associated with worse prognosis in pancreatic ductal adenocarcinoma. Pancreas 43, 578-583.

Stanley, P., Vivona, G., Atkinson, P.H., 1984. 1H NMR spectroscopy of carbohydrates from the G glycoprotein of vesicular stomatitis virus grown in parental and Lec4 Chinese hamster ovary cells. Arch Biochem Biophys 230, 363-374.

Stark, A.P., Sacks, G.D., Rochefort, M.M., Donahue, T.R., Reber, H.A., Tomlinson, J.S., Dawson, D.W., Eibl, G., Hines, O.J., 2016. Long-term survival in patients with pancreatic ductal adenocarcinoma. Surgery 159, 1520-1527.

Steinhauer, D.A., Domingo, E., Holland, J.J., 1992. Lack of evidence for proofreading mechanisms associated with an RNA virus polymerase. Gene 122, 281-288.

Stojdl DF, Lichty BD, tenOever BR, Paterson JM, Power AT, Knowles S, Marius R, Reynard J, Poliquin L, Atkins H, Brown EG, Durbin RK, Durbin JE, Hiscott J, JC, B., 2003. VSV strains with defects in their ability to shutdown innate immunity are potent systemic anti-cancer agents. Cancer Cell 4, 263-275.

Stojdl, D.F., Lichty, B.D., Knowles, S., Marius, R., Atkins, H., Sonenberg, N., Bell, J.C., 2000. Exploiting tumor-specific defects in the interferon pathway with a previously unknown oncolytic virus. Nat Med 6, 821-825.

Svyatchenko, V.A., Ternovoy, V.A., Kiselev, N.N., Demina, A.V., Loktev, V.B., Netesov, S.V., Chumakov, P.M., 2017. Bioselection of coxsackievirus B6 strain variants with altered tropism to human cancer cell lines. Arch Virol 162, 3355-3362.

Swayden, M., Iovanna, J., Soubeyran, P., 2018. Pancreatic cancer chemo-resistance is driven by tumor phenotype rather than tumor genotype. Heliyon 4, e01055.

Tesh, R.B., Peralta, P.H., Johnson, K.M., 1969. Ecologic studies of vesicular stomatitis virus. I. Prevalence of infection among animals and humans living in an area of endemic VSV activity. Am J Epidemiol 90, 255-261.

Thomas, C.E., Ehrhardt, A., Kay, M.A., 2003. Progress and problems with the use of viral vectors for gene therapy. Nat Rev Genet 4, 346-358.

Trottier, M.D., Lyles, D.S., Reiss, C.S., 2007. Peripheral, but not central nervous system, type I interferon expression in mice in response to intranasal vesicular stomatitis virus infection. Journal of neurovirology 13, 433-445.

van den Pol, A., Dalton, K., Rose, J., 2002. Relative neurotropism of a recombinant rhabdovirus expressing a green fluorescent envelope glycoprotein. J Virol 76, 1309-1327.

van den Pol, A.N., Davis, J.N., 2013. Highly attenuated recombinant vesicular stomatitis virus VSV-12'GFP displays immunogenic and oncolytic activity. J Virol 87, 1019-1034.
Verma, I.M., Weitzman, M.D., 2005. Gene therapy: twenty-first century medicine. Annu Rev Biochem 74, 711-738.

von Kobbe, C., van Deursen, J.M., Rodrigues, J.P., Sitterlin, D., Bachi, A., Wu, X., Wilm, M., Carmo-Fonseca, M., Izaurralde, E., 2000. Vesicular stomatitis virus matrix protein inhibits host cell gene expression by targeting the nucleoporin Nup98. Mol.Cell 6, 1243-1252.

von Messling V, Cattaneo, R., 2004. Toward novel vaccines and therapies based on negative-strand RNA viruses. Current Topics in Microbiology and Immunology 283.
Wang, B.X., Rahbar, R., Fish, E.N., 2011a. Interferon: current status and future prospects in cancer therapy. J Interferon Cytokine Res 31, 545-552.

Wang, Z., Li, Y., Ahmad, A., Banerjee, S., Azmi, A.S., Kong, D., Sarkar, F.H., 2011b. Pancreatic cancer: understanding and overcoming chemoresistance. Nat Rev Gastroenterol Hepatol 8, 27-33.

Wennier, S., Li, S., McFadden, G., 2011. Oncolytic virotherapy for pancreatic cancer. Expert Rev Mol Med 13, e18.

Wertz, G.W., Moudy, R., Ball, L.A., 2002. Adding genes to the RNA genome of vesicular stomatitis virus: positional effects on stability of expression. J Virol 76, 7642-7650.
Whitt, M.A., Rose, J.K., 1991. Fatty acid acylation is not required for membrane fusion activity or glycoprotein assembly into VSV virions. Virology 185, 875-878.

Wolfgang, C.L., Herman, J.M., Laheru, D.A., Klein, A.P., Erdek, M.A., Fishman, E.K., Hruban, R.H., 2013. Recent progress in pancreatic cancer. CA Cancer J Clin 63, 318-348.
Wollmann G, Rogulin V, Simon I, Rose JK, AN, v.d.P., 2010. Some attenuated variants of vesicular stomatitis virus show enhanced oncolytic activity against human glioblastoma cells relative to normal brain cells. J Virol 84, 1563-1573.

Wollmann G, T.P., van den Pol AN., 2005. Targeting human glioblastoma cells: comparison of nine viruses with oncolytic potential. J Virol 79, 6005-6022.

Yan, W., Kitzes, G., Dormishian, F., Hawkins, L., Sampson-Johannes, A., Watanabe, J., Holt, J., Lee, V., Dubensky, T., Fattaey, A., Hermiston, T., Balmain, A., Shen, Y., 2003. Developing novel oncolytic adenoviruses through bioselection. J Virol 77, 2640-2650.
Yee, J.K., Friedmann, T., Burns, J.C., 1994. Generation of high-titer pseudotyped retroviral vectors with very broad host range. Methods Cell Biol 43 Pt A, 99-112.

Yu, J.H., Schaffer, D.V., 2006. Selection of novel vesicular stomatitis virus glycoprotein variants from a peptide insertion library for enhanced purification of retroviral and lentiviral vectors. J Virol 80, 3285-3292.

Zainutdinov, S.S., Kochneva, G.V., Netesov, S.V., Chumakov, P.M., Matveeva, O.V., 2019. Directed evolution as a tool for the selection of oncolytic RNA viruses with desired phenotypes. Oncolytic Virother 8, 9-26.

Zhang, K.X., Matsui, Y., Hadaschik, B.A., Lee, C., Jia, W., Bell, J.C., Fazli, L., So, A.I., Rennie, P.S., 2010. Down-regulation of type I interferon receptor sensitizes bladder cancer cells to vesicular stomatitis virus-induced cell death. Int J Cancer 127, 830-838.